THE INFLUENCE OF LATITUDE AND SEASON ON PHOTOCHEMICAL SMOG FORMATION

Jørgen Schjoldager
B. S., The Technical University of Norway, 1968

A thesis submitted to the faculty
of the Oregon Graduate Center
in partial fulfillment of the
requirements for the degree
Master of Science
in
Environmental Technology

This thesis has been examined and approved by the following Committee:

James J. Huntzicker, Thesis Advisor
Associate Professor

Edward J. Baum
Associate Professor

Frank M. Hauser
Associate Professor

TABLE OF CONTENTS

APPENDICES

ABSTRACT

A generalized photochemical smog mechanism is used to evaluate the photochemical smog potential due to solar radiation for different seasons and different locations in the northern hemisphere. This is done by expressing the photolytic rate constants as functions of the ground level solar flux and expressing the solar zenith angle as a function of latitude, time of year and time of day. The irradiation of a specified mixture of hydrocarbons and nitrogen oxides is simulated at local times 0900 - 1200 and 0600 - 0900. The hydrocarbon mixture is chosen to correspond approximately to that of an urban atmosphere.

The differential rate equations are solved using a modified Hamming's predictor-corrector method, and reasonable computing times are obtained by applying the pseudosteady state assumption to the reactive radicals.

The study shows that during the summer months the potential for photochemical smog formation extends far north, well beyond 60°N. After three hours of simulated irradiation in June the ozone level at 60°N was 75-80% of that at 34°N. In the spring and fall the region in which photochemical smog may be expected narrows. At equinox the ozone concentration at 60°N was 35-40% of that at 34°N.

Locations at latitudes 60°N and higher can therefore not be excluded as future problem areas with regard to photochemical smog.

The concentration levels of peroxyacylnitrates and aldehydes were well correlated with the ozone levels, and so was the time required to obtain maximum concentration of nitrogen dioxide in the photochemical cycle. The magnitude of the NO_2 peak was not much affected by the variations in latitude and season, and the magnitude of the NO_2 peak decreased slightly when the solar flux increased.

LIST OF FIGURES

LIST OF TABLES

1. INTRODUCTION

The first important step towards the understanding of photochemical smog formation was made in the 1950's by Haagen-Smit and co-workers (1952, 1956). They showed that ozone and other oxidants causing symptoms similar to those experienced in the Los Angeles air could be produced by the laboratory irradiation of low concentrations of nitrogen dioxide and organic compounds including hydrocarbons. They also showed that ozone is produced by irradiation of automobile exhaust. Later in the decade other investigators (Schuck et al., 1958, Doyle et al., 1958 and Stephens et al., 1960) showed that the irradiation products would lead to eye irritation, plant damage and visibility reduction (aerosol formation).

The next important step in the description of photochemical smog was made in 1961 when Leighton published his book "Photochemistry of Air Pollution". This is still an important source book for investigators of photochemical smog.

In the 1960's a large amount of experimental work regarding various aspects of photochemical smog formation was done, and most of this work has been summarized by Altshuller and Bufalini (1971). Extensive experimental work is still going on.

Photochemical models were introduced in the late 1960's and one of the first was that of Friedlander and Seinfeld (1969). A photochemical model is a set of elementary chemical reactions with their corresponding rate constants. In the beginning these models were very simple; that of Friedlander and Seinfeld had only seven chemical equations relating seven

components. During the 1970's the photochemical models have increased both in complexity and accuracy. The work has been done along two main lines, the development of specific and generalized mechanisms.

The specific mechanisms describe as accurately as possible the reactions between a given, relatively small number of initial components. The chemistry is quite detailed and the number of reactions (steps) becomes large. For example Westberg and Cohen (1969) used 71 steps to describe the irradiation of propylene, NO and NO_2 in air. Hecht and Seinfeld (1972) used 81 steps for the same mixture. Hesstvedt et al. (1976) used 110 steps to describe the irradiation of NO, NO_2, etylene, propylene, n-butane and n-hexane. In probably the most extensive modeling effort so far, that of Demerjian, Kerr and Calvert (1974), ca. 500 steps were used to model the irradiation of NO, NO_2, CO, formaldehyde, acetaldehyde, propylene, trans-2-butene, iso-butene, methane and n-butane. However, the larger the mechanisms grow, the more rate constants have to be determined and, in practice, the uncertainty of these will limit the usefulness of the detailed mechanisms.

It was recognized early that in a real, polluted atmosphere the number of reactive components was so large that a complete chemical description would be impossible. As a result, generalized models have been developed. In these the number of steps is kept low, normally well below 50, and some of the components are "lumped", i.e., they describe classes rather than specific compounds. For example, all hydrocarbons may be lumped into i classes HC_i and all organic radicals may be denoted R. Several generalized models are summarized in Table 1. The purpose of the

Table 1. Summary of some generalized photochemical smog mechanisms

Authors	No. of steps	Total no. of components	No. of organic radicals	No. of HC-classes	No. of solar dependent reactions	No. of stoichiometric coeff.
Friedlander & Seinfeld (1969)	7	7	1	1	1	0
Eschenroeder & Martinez (1972)	12	10	1	1	2	0
Hecht & Seinfeld (1972)	15	15	1	1	2	6
Reynolds, Roth & Seinfeld (1973)	19	17	1	2	2	7
Hecht, Seinfeld & Dodge (1974)	39	23	3	4	4	2
Whitten & Hogo (1976)	35	24	2	4	5	0

generalized models is to handle a variety of mixtures of hydrocarbons and nitrogen oxides in a much simpler way than the specific models do while maintaining the characteristic features of the process. If the photochemical model is part of an airshed model, the savings in computer time can be considerable. Also, because many rate constants are uncertain anyway, an actual comparison between a computer simulation and measurements might as well be made by varying the rate constants within their limits of uncertainty.

For the purpose of examining certain effects, such as how the ozone build-up is affected by changes in the ratio between hydrocarbon and nitrogen oxides or between NO and NO_2, a fairly simple model can be as useful as an extensive one.

In many of the proposed general mechanisms stoichiometric coefficients* have to be quantified. This is considered a disadvantage, especially if the coefficients have no physical meaning. The number of stoichiometric coefficients should therefore be kept as low as possible.

The photochemical models are fairly well established regarding reactions in the gas phase. The characteristic changes in concentrations of hydrocarbons, nitric oxide, nitrogen dioxide, ozone and peroxyacylnitrates are well reproduced by photochemical models. Recently reactions of sulfur dioxide have also been included (Durbin, Hecht and Whitten, 1975). What is not so well established is the aerosol formation; the relative importance of the different aerosol processes, mechanisms for the gas-to-particle conversion etc. Here much experimental work has still to be done until reliable mathematical models can be established. The present

*The coefficients α and β in Appendix A are examples of stoichiometric coefficients.

photochemical aerosol models are not well suited to reproduce aerometric data; they are rather used to study the sensitivity of the predictions to variations of important input parameters (Chu and Seinfeld, 1975).

1.1 Purpose of this work

The purpose of this work is to examine the influence of latitude and season on the formation of photochemical smog. This is done by expressing the solar radiation dependent rate constants as functions of latitude, time of year and time of day. An initial mixture of nitrogen oxides and hydrocarbons is specified, and an irradiation experiment is simulated using solar radiation calculated for different latitudes, seasons and times of day. The time dependencies of the reactive species are computed using one of the generalized photochemical models, that of Hecht, Seinfeld and Dodge (1974). This model is given in Appendix A.

In chapter 2 general aspects of photochemical smog mechanisms are reviewed, and the choice of the model is discussed. In chapter 3 the rate constants are reviewed and in chapter 4 the solar flux as a function of season and latitude is outlined. Chapter 5 deals with solution methods for the differential equations.

2. PHOTOCHEMICAL REACTION MECHANISMS

The purpose of a photochemical reaction mechanism is to simulate the behavior of reactive pollutants in the atmosphere or in a reaction chamber. The complexity of the mechanism will depend on the degree of detail required, which aspects are of specific interest and what kind of measurements are available for comparison. A minimum requirement is to reproduce the basic chemical features of the photochemical smog cycle which include:

- Photochemical dissociation of NO_2 and other light absorbing gases.
- Rapid conversion of NO to NO_2.
- Oxidation of hydrocarbons to aldehydes.
- Ozone concentrations above background level.
- Formation of peroxyacylnitrates.

Figure 1 shows an example of the photochemical smog cycle from irradiation of NO, NO_2 and propylene in air. Other characteristics of the photochemical smog cycle which may be included in the reaction mechanisms include:

- Formation of nitrous acid, organic nitrites, nitric acid and organic nitrates.
- Formation of hydrogen peroxide.
- Oxidation of hydrocarbons to ketones and acids.
- Oxidation of sulfur dioxide to sulfuric acid.
- Gas-to-particle conversion.

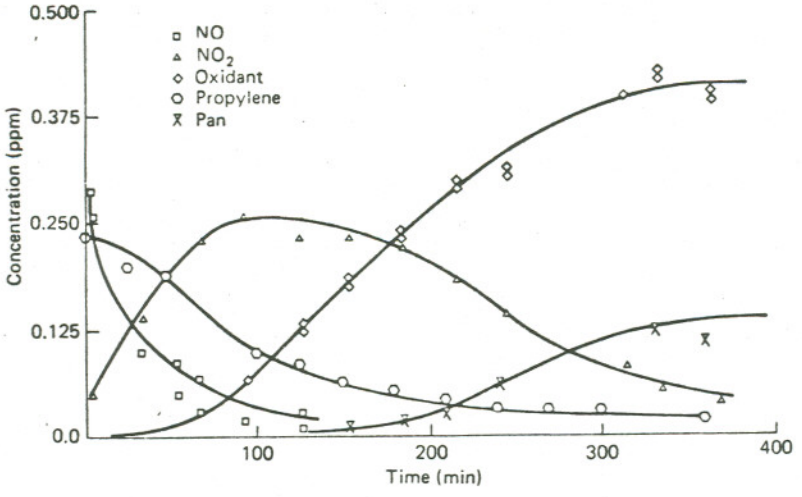

Figure 1. Experimental data on the photolysis of an initial mixture of 0.25 ppm propylene, 0.26 ppm NO, and 0.05 ppm NO_2 in air. Experiment conducted by S. L. Kopczynski of the U. S. Environmental Protection Agency. Source: Seinfeld (1975).

There is a large number of books and papers describing photochemical smog mechanisms. The brief review given here is mainly based on Seinfeld (1975), Demerjian and Schere (1975), and Hesstvedt, Hov and Isaksen (1976).

2.1 Photolytic reactions

The photolytic reactions used in photochemical models are written in the form

$$A + h\nu \rightarrow bB + cC + \ldots$$

with the corresponding rate expression

$$-\frac{d[A]}{dt} = \frac{1}{b}\frac{d[B]}{dt} = \frac{1}{c}\frac{d[C]}{dt} = k\,[A]$$

The rate constant k is a function of the intensity and wavelength distribution of the light, the absorption properties of the molecule A and the probability that the excited molecule A* dissociates to form the products B, C, ... The parameters involved are the photon flux, absorption coefficient (extinction coefficient, absorption crossection) and quantum yield. These are discussed in more detail in Chapter 3 and 4, and numbers are given in Table 4 and Appendices B and E.

Because of the ozone layer in the stratosphere practically no radiation of wavelength less than 290 nm (2900 Å) reaches the earth's surface. Therefore only absorption above this wavelength is considered in this report.

2.1.1 Nitrogen dioxide

The photodissociation of NO_2 is given by

$$NO_2 + h\nu \rightarrow NO + O(^3P)$$

indicating that the O atom formed is in the triplet-P state. This reaction is the main source of $O(^3P)$ during photochemical smog episodes. The wavelength interval of importance is 290-440 nm. Nitrogen dioxide absorbs at higher wavelengths than 440 nm, but no NO and $O(^3P)$ are formed because of the low energy of radiation.

2.1.2 Nitrous acid

The photodissociation of HNO_2 is given by

$$HNO_2 + h\nu \rightarrow NO + OH \ .$$

This reaction is one of the important sources of OH radicals. The wavelength interval of interest is 300-400 nm; above 400 nm no light

absorption takes place. The rate constant for HNO_2 dissociation is about one order of magnitude less than that of NO_2 in the lower troposphere.

2.1.3 Hydrogen peroxide

The photodissociation of H_2O_2 is given by

$$H_2O_2 + h\nu \rightarrow 2OH \ .$$

This is another source of OH radicals. The wavelength interval of interest is 290-370 nm; above 370 nm no absorption takes place. The rate constant for H_2O_2 dissociation is about two orders of magnitude less than that of NO_2.

2.1.4 Formaldehyde

There are two reactions describing the photodissociation of HCHO:

$$HCHO + h\nu \rightarrow H + HCO$$

$$HCHO + h\nu \rightarrow H_2 + CO$$

The wavelength interval of interest is 290-360 nm for both reactions. The quantum yield for the first one is the larger for $\lambda<310$ nm, while that of the second one is the larger for 310 nm $<\lambda<360$ nm. The rate constant of the second reaction is roughly twice as large as that of the first one, and both are about two orders of magnitude less than that of NO_2.

2.1.5 Acetaldehyde

The photodissociation of acetaldehyde is similar to that of formaldehyde:

$$CH_3CHO + h\nu \rightarrow CH_3 + HCO$$

$CH_3CHO + h\nu \rightarrow CH_4 + CO$

For both reactions the interval 290-340 nm is of interest. These rate constants are more uncertain than those for formaldehyde, but they are about three orders of magnitude less than that of NO_2.

2.1.6 Ozone

The two most important reactions are:

$O_3 + h\nu \rightarrow O(^3P) + O_2$

$O_3 + h\nu \rightarrow O(^1D) + O_2$

where $O(^1D)$ means the first-excited electronic state of the O atom. The first of these reactions takes place for 310 nm $<\lambda<$ 350 nm and 450 nm $<\lambda<$ 750 nm. The second one takes place for 290 nm $<\lambda<$ 310 nm. The first reaction has a larger rate constant than the second, but the second is more important because $O(^1D)$ reacts with water vapor forming OH radicals:

$O(^1D) + H_2O \rightarrow 2OH$.

2.1.7 Other components

There are several other light-absorbing components in the atmosphere which may be included in specific mechanisms but are normally not included in generalized mechanisms. Some of these are

$HNO_3 + h\nu \rightarrow OH + NO_2 \quad \lambda < 360$ nm

$O_3 + h\nu \rightarrow O_2(^1\Delta) + O(^3P) \quad \lambda < 350$ nm

$N_2O + h\nu \rightarrow O(^1D) + N_2 \quad \lambda < 320$ nm

$NO_3 + h\nu \rightarrow NO + O_2 \quad \lambda < 580$ nm

$N_2O_5 + h\nu \rightarrow NO_2 + NO_3 \quad \lambda < 380$ nm

Other classes of components can also dissociate, for example, peroxides, alkyl nitrites, alkyl nitrates and higher aldehydes:

$ROOH + h\nu \rightarrow RO + OH$ (peroxides)

$RONO + h\nu \rightarrow RO + NO$ (alkyl nitrites)

$RONO_2 + h\nu \rightarrow RO + NO_2$ (alkyl nitrates)

$RCHO + h\nu \rightarrow R + HCO$ (higher aldehydes)

The rate constants for these reactions are generally not well-known.

2.2 The basic photochemical cycle of NO_2, NO and O_3

This cycle is described by the three equations:

$$NO_2 + h\nu \xrightarrow{k_1} NO + O(^3P) \quad (1)$$

$$O(^3P) + O_2 + M \xrightarrow{k_2} O_3 + M \quad (2)$$

$$O_3 + NO \xrightarrow{k_3} NO_2 + O_2 \quad (3)$$

Ozone is formed by reactions 1 and 2 and consumed by reaction 3. If both $O(^3P)$ and O_3 are assumed to be in pseudo-stationary state (steady state), i.e., they are consumed at the same rate as they are produced, then the ozone concentration can be expressed as a function of the NO_2/NO ratio only

$$[O_3] = \frac{k_1}{k_3} \frac{[NO_2]}{[NO]}$$

Especially in the first phase of the photochemical cycle (before $[NO_2]$ peaks) the ozone concentration is quite well predicted from this equation, and the measurement of the $[NO_2]/[NO]$ ratio together with ozone can be used to estimate k_1, provided k_3 is known (O'Brien, 1974).

2.3 Inorganic reactions

Reactions involving CO, CO_2, and molecules and radicals containing only hydrogen, nitrogen, and oxygen can be called inorganic reactions. There is a large number of possible reaction paths. For example Demerjian, Kerr and Calvert (1974) list ca. 95 inorganic reactions. A much smaller number is normally used in the generalized mechanisms. In a summary by Seinfeld (1975) less than 20 reactions are included, and these are shown in Table 2. The inorganic photolytic reactions and the basic photochemical cycle are not included.

The reactions involve formation and consumption of nitrogen pentoxide (N_2O_5), nitrogen trioxide (NO_3), nitrous and nitric acid, hydrogen peroxide and the oxidation of carbon monoxide to carbon dioxide. The reactions 15-17 are especially important; they show oxidation of NO to NO_2 without consumption of ozone and without net loss of radicals. These reactions and similar ones involving organic molecules and radicals are the key to the understanding of the ozone buildup during photochemical smog episodes.

2.4 Hydrocarbon reactions

Even if the reactions described so far are sufficient in principle to explain the formation of ozone, the necessary concentrations of CO would be far above those experienced even during severe pollution episodes. In other words, CO causes an air pollution problem by itself at far lower concentrations than necessary for it to be an important factor in photochemical smog. However, the presence of organic molecules, especially

Table 2. Thermal inorganic reactions of importance for photochemical smog formation

$O(^3P) + NO_2 \rightarrow NO + O_2$	(1)
$O(^3P) + NO_2 + M \rightarrow NO_3 + M$	(2)
$NO_3 + NO \rightarrow 2NO_2$	(3)
$O(^3P) + NO + M \rightarrow NO_2 + M$	(4)
$NO_3 + NO_2 \rightarrow N_2O_5$	(5)
$N_2O_5 \rightarrow NO_3 + NO_2$	(6)
$NO_2 + O_3 \rightarrow NO_3 + O_2$	(7)
$N_2O_5 + H_2O \rightarrow 2HNO_3$	(8)
$HNO_3 + NO \rightarrow HNO_2 + NO_2$	(9)
$HNO_3 + HNO_2 \rightarrow 2NO_2 + H_2O$	(10)
$NO + NO_2 + H_2O \rightarrow 2HNO_2$	(11)
$2HNO_2 \rightarrow NO + NO_2 + H_2O$	(12)
$OH + NO_2 \rightarrow HNO_3$	(13)
$OH + NO \rightarrow HNO_2$	(14)
$OH + CO \rightarrow CO_2 + H$	(15)
$H + O_2 + M \rightarrow HO_2 + M$	(16)
$HO_2 + NO \rightarrow NO_2 + OH$	(17)
$HO_2 + HO_2 \rightarrow H_2O_2 + O_2$	(18)

hydrocarbons, explains the formation of ozone and other characteristics of photochemical smog at typical concentrations of the primary pollutants in the polluted atmosphere.

The different hydrocarbons are rated according to their "reactivity", a term which is in wide use but is not completely defined. Several reactivity scales have been proposed. These scales are based on nitric oxide conversion (Glasson and Tuesday, 1970), hydrocarbon disappearance (Altshuller and Bufalini, 1971) or other characteristics of photochemical smog, for example eye irritation or secondary aerosol formation. A reactivity scale by Dimitriades (1974) based on a re-examination of previous scales has recently received attention, but the EPA has not yet "authorized" any reactivity scale.

From a photochemical modeling point of view the term reactivity should be based on actual rate constants for the most important reactions involving the hydrocarbons. Such a scale has in fact recently been proposed by Pitts et al. (1976) based on reaction rates with the OH radical, which is considered to be the most important species with respect to primary hydrocarbon consumption.

In this chapter some general mechanisms of the reactions with OH, O and O_3 are presented. Many of the details of the hydrocarbon reactions are still a matter of speculation. A variety of reaction paths has been presented by Demerjian, Kerr and Calvert (1974).

2.4.1 Olefins

The olefins are generally the most reactive of the hydrocarbons.

Hydroxyl radicals react by addition at the double bond:

$$CH_3CH{=}CH_2 + OH \rightarrow CH_3\dot{C}HCH_2OH$$

$$\rightarrow CH_3\underset{OH}{C}\dot{H}CH_2 \quad .$$

The radicals formed may decompose to form aldehyde and an alkyl radical

$$CH_3\dot{C}HCH_2OH \rightarrow CH_3\dot{C}H_2 + HCHO \quad ,$$

and the alkyl radical reacts with oxygen forming a peroxyalkyl radical

$$CH_3\dot{C}H_2 + O_2 \rightarrow CH_3CH_2OO\cdot \quad .$$

Another reaction path is decomposition to form an unsaturated radical and water

$$CH_3\dot{C}HCH_2OH \rightarrow CH_2{=}CH{-}\dot{C}H_2 + H_2O$$

followed by the addition of oxygen to form an unsaturated peroxy radical

$$CH_2{=}CH{-}\dot{C}H_2 + O_2 \rightarrow CH_2{=}CH{-}CH_2OO\cdot \quad .$$

Oxygen atoms react with olefins forming an excited epoxide which decomposes to an alkyl and an acyl radical

$$CH_3{-}CH{=}CH{-}CH_3 + O \rightarrow CH_3{-}\underset{\diagdown O \diagup}{CH}{-}CH{-}CH_3$$

$$CH_3{-}\underset{\diagdown O \diagup}{CH}{-}CH{-}CH_3 \rightarrow CH_3CH_2 + CH_3\overset{\overset{O}{\|}}{C}\cdot$$

These two radicals can both add oxygen forming a peroxyalkyl radical and a peroxyacyl radical

$$CH_3\dot{C}H_2 + O_2 \rightarrow CH_3CH_2OO\cdot$$

$$CH_3\overset{O}{\overset{\|}{C}}\cdot + O_2 \rightarrow CH_3\overset{O}{\overset{\|}{C}}-OO\cdot$$

Ozone reacts with olefins forming an ozonide which may decompose into aldehyde and organic radicals

$$CH_3-CH=CH_2 + O_3 \rightarrow CH_3-\underset{\displaystyle O}{\overset{\displaystyle O}{\overset{\diagup\diagdown}{CH}}}-\underset{\displaystyle O}{\overset{\displaystyle O}{\overset{\diagup\diagdown}{CH_2}}}$$

$$CH_3-\underset{\displaystyle O}{\overset{\displaystyle O}{\overset{\diagup\diagdown}{CH}}}-\underset{\displaystyle O}{\overset{\displaystyle O}{\overset{\diagup\diagdown}{CH_2}}} \rightarrow HCHO + CH_3\dot{C}HOO\cdot$$

$$CH_3\dot{C}HOO\cdot \rightarrow CH_3O\cdot + H\dot{C}O \quad .$$

A simple explanation why reaction with OH gives one radical and reaction with O or O_3 gives two radicals, is that OH has an odd number of electrons while O and O_3 have even numbers of electrons. Therefore OH produces an odd number of radicals (normally one) while O and O_3 produce an even number (normally zero or two).

2.4.2 Paraffins

Paraffins react with OH radicals and O atoms, but not with ozone. The reaction with OH gives an alkyl radical:

$$C_4H_{10} + OH \rightarrow C_3H_7\dot{C}H_2 + H_2O \quad .$$

The reaction with O gives an OH radical and an alkyl radical

$$C_4H_{10} + O \rightarrow C_3H_7\dot{C}H_2 + OH \quad .$$

Again the alkyl radicals react with atmospheric oxygen to form peroxyalkyl radicals:

$$C_3H_7\dot{C}H_2 + O_2 \rightarrow C_4H_9OO\cdot \quad .$$

2.4.3 Aromatics

The mechanisms for aromatic reactions are less known than those of olefins and paraffins. Benzene itself has low reactivity, and it is not clear to what extent the reactions with aromatics lead to ring opening. It has been proposed that alkyl-substituted compounds such as toluene or xylene react the same way as paraffins, and unsaturated compounds (e.g., styrene) react as olefins.

2.5 Aldehyde reactions

As pointed out in paragraph 2.4 aldehydes are formed by reaction between olefins and atomic oxygen or ozone. In addition it has been shown that aldehydes are emitted as primary pollutants in automobile exhaust.

Aldehydes photodissociate as pointed out in paragraph 2.1. Aldehydes are also attacked by radicals. The reaction with OH gives an acyl radical and water:

$$CH_3CHO + OH \rightarrow CH_3\overset{\overset{O}{\|}}{C}\cdot + H_2O \quad .$$

The reaction with O gives an OH radical and an acyl radical:

$$CH_3CHO + O \rightarrow CH_3\overset{\overset{O}{\|}}{C}\cdot + OH \quad .$$

and the acyl radicals react with oxygen to form peroxyacyl radicals:

$$CH_3\overset{\overset{O}{\|}}{C}\cdot + O_2 \rightarrow CH_3\overset{\overset{O}{\|}}{C}OO\cdot \quad .$$

2.6 Free radical reactions

The free radicals formed by the hydrocarbon oxidation can react in a variety of ways, both with each other and with other molecules. The reactions with NO, NO_2 and O_2 are of most interest. Some reactions with O_2 have already been mentioned in paragraphs 2.4 and 2.5.

The reactions with NO are very important because they show an oxidation path of NO to NO_2 without consumption of ozone, thus promoting ozone formation by reactions 1 and 2 in the basic photochemical cycle. Peroxyalkyl radicals are reduced to alkoxyl radicals, and peroxyacyl radicals are reduced to acylate radicals:

$$C_2H_5OO\cdot + NO \rightarrow C_2H_5O\cdot + NO_2$$

$$CH_3\overset{\overset{O}{\|}}{C}OO\cdot + NO \rightarrow CH_3\overset{\overset{O}{\|}}{C}O\cdot + NO_2 \quad .$$

Organic nitrites are also formed:

$$C_2H_5O + NO \rightarrow C_2H_5ONO \quad .$$

Reactions with NO_2 are also important, especially with peroxyacyl radicals forming peroxyacylnitrates of which PAN (peroxyacetylnitrate) is the best known:

$$CH_3\overset{\overset{O}{\|}}{C}OO\cdot + NO_2 \rightarrow CH_3\overset{\overset{O}{\|}}{C}OONO_2 \quad .$$

Other organic nitrates are also formed:

$$C_2H_5O + NO_2 \rightarrow C_2H_5ONO_2 \quad .$$

Finally free radicals may decompose or react with other radicals forming stable products or new radicals. The acylate radical is unstable and decomposes to form an alkyl radical and carbon dioxide:

$$CH_3\overset{\overset{O}{\|}}{C}O\cdot \rightarrow \dot{C}H_3 + CO_2 \quad .$$

The alkoxyl radical may react with oxygen and decompose to form an aldehyde and the HO_2 radical:

$$C_2H_5O\cdot + O_2 \rightarrow CH_3CHO\cdot + HO_2 \quad .$$

The radical reactions are the propagating reactions in the photochemical smog cycle. They convert NO to NO_2 and are in part regenerated by reactions with atmospheric oxygen.

2.7 Lumped reactions

In the generalized reaction mechanisms lumped reactions are used to describe certain reaction types. For example the reaction

$$ROO\cdot + NO \rightarrow RO\cdot + NO_2$$

lumps all peroxyalkyl radicals into ROO and all alkoxyl radicals into RO·. Another lumped reaction is

$$HC_1 + OH \rightarrow ROO\cdot + HC_4$$

where HC_1 means olefins and HC_4 aldehydes.

To assign a "correct" rate constant to a lumped reaction is not a straightforward task. The relative concentrations of the individual components comprising a lumped species may vary with time due to reactivity differences. A method of updating lumped rate constants has been given by Hecht, Liu and Whitney (1974).

2.8 Oxidation of sulfur dioxide

Mechanisms for SO_2 oxidation have recently been included in photochemical models. This agrees with the observed increase in SO_2 oxidation rates when nitrogen oxides and hydrocarbons are present. Mechanisms for SO_2 oxidation are discussed by Durbin, Hecht and Whitten (1975) and Finlayson and Pitts (1976). There are many similarities between SO_2 oxidation and NO oxidation. In both cases radicals play an important role:

$$HO_2 + SO_2 \rightarrow SO_3 + OH$$
$$ROO + SO_2 \rightarrow SO_3 + RO$$
$$NO_3 + SO_2 \rightarrow SO_3 + NO_2 \quad .$$

Peroxides of sulfur may also be formed as intermediates:

$$SO_2 + OH \rightarrow HSO_3\cdot$$
$$HSO_3\cdot + O_2 \rightarrow HSO_5\cdot$$
$$HSO_5\cdot + NO \rightarrow HSO_4\cdot + NO_2$$
$$HSO_4\cdot + NO_2 + H_2O \rightarrow H_2SO_4 + HNO_3 \quad .$$

The gas-to-particle conversion is closely related to the SO_2 oxidation, and H_2SO_4 is one of the species entering the particulate

phase quite easily.

2.9 Choice of model

For the study of the influence of solar radiation due to latitude, season and time of day, the model of Hecht, Seinfeld and Dodge (1974) (also described by Hecht, Roth and Seinfeld (1973) and by Hecht, Liu and Whitney (1974)) was chosen because it treated the solar radiation in more detail than other generalized models. The mechanism is shown in Appendix A. It has 39 reactions, four of which are solar radiation dependent. It has four classes of organics: olefins, paraffins, aromatics and aldehydes. It has incorporated most of the main types of gaseous photochemical reactions. Two stoichiometric coefficients, α and β, have to be specified, but both have a physical meaning. The coefficient α is the fraction of double bonded carbon not in a terminal position in a monoolefin. The value of α is thus 0, 0.5 or 1. The coefficient β is the fraction of aldehydes which are not formaldehyde, i.e., a number between 0 and 1 which must be empirically determined.

A recent generalized model by Whitten and Hogo (1976) uses types of carbon bonds rather than hydrocarbon classes. Different bond types - single bonds, slow double bonds, fast double bonds and carbonyl bonds - are treated separately. The approach seems interesting, but the model was received too late for use in this work.

3. RATE CONSTANTS

As a part of the Climatic Impact Assessment Program (CIAP, 1975) many rate constants for reactions taking place in the atmosphere were critically reviewed. The results have been edited by Hampson and Garvin (1975).

In photochemical reaction schemes some of the reactions are thermal and some are photochemical. Thus some of the rate constants are temperature dependent and some are dependent on the intensity and wavelength distribution of light.

3.1 Thermal rate constants

The temperature dependency is most often given by the Arrhenius expression

$$k = A \exp(-E/RT) \qquad (3.1)$$

where the activation energy E may be positive or negative; i.e., the reaction rate may increase or decrease with increasing temperature. The temperature dependency for a variety of reactions is given by Hampson and Garvin (1975) and by Hesstvedt (1975).

The effect of temperature variations on the ozone formation has been studied by Hecht, Roth and Seinfeld (1973) using the Hecht and Seinfeld (1972) photochemical model. The activation energies (E) were estimated, and the temperature range 264°K - 315°K was examined. Their conclusion was that the rate of ozone formation increased sharply when the temperature was raised from 264°K to 290°K, while further increases had little effect on the rate of ozone formation.

The thermal rate constants have recently been reviewed by Whitten and Hogo (1976) and their values were used in this study, except for the reactions

OH + hydrocarbons →

where the most recent values by Lloyd et al. (1976) were used. For those lumped reactions which specifically pertain to the Hecht, Seinfeld and Dodge scheme, the originally proposed rate constants have not been changed.

No temperature dependency is included, and therefore the results are probably of value only for ambient temperatures above ca. 290°K (ca. 17°C). The rate constants used are listed in Appendix A.

3.2 Photolytic rate constants

The photolytic rate constants are most often calculated using the formula

$$k = 2.303 \int_{\lambda_1}^{\lambda_2} J_\lambda \varepsilon_\lambda \phi_\lambda d\lambda \qquad (3.2)$$

J_λ is called the actinic irradiance and is described by Leighton (1961). The equations and assumptions expressing J_λ are summarized in Chapter 5.

The parameter ε_λ is the extinction coefficient, given in the units 1 mole^{-1} cm^{-1}. Sometimes the term absorption coefficient α_λ is used. Geophysicists modeling the stratosphere often prefer the term crossection σ_λ (cm^2 molecule^{-1}). The number 2.303 enters equation 3.2 because the extinction coefficient ε_λ has base 10. Normally the values for the crossection σ_λ are given with base e;

in that case the number 2.303 vanishes.

$\emptyset_\lambda$ is the quantum yield expressing the number of a particular atom or molecule formed per photon absorbed. For example for the reaction

$$NO_2 + h\nu \rightarrow NO + O(^3P)$$

the quantum yield gives the number of NO or $O(^3P)$ atoms formed per photon absorbed by NO_2.

Because J_λ, ε_λ and $\emptyset_\lambda$ are normally given for discrete intervals the integral in equation (3.2) is replaced by a finite summation:

$$k = 2.303 \sum_\lambda J_\lambda \varepsilon_\lambda \emptyset_\lambda \qquad (3.3)$$

The extinction coefficients and quamtum yields for atmospheric pollutants have been reviewed by Hampson and Garvin (1975) and by Demerjian and Schere (1975). The extinction coefficients for H_2O_2 for wavelengths above 290 nm and the quantum yield for radical formation from acetaldehyde are based on measurements from 1929 and 1942 respectively (Urey, Dawsey and Rice, 1929 and Blacet and Loeffler, 1942), and new measurements should be of interest.

In this work the references given by Demerjian and Schere (1975) are used, with the modifications in J_λ mentioned in chapter 5. The values for ε_λ and $\emptyset_\lambda$ are given in Appendix B. For HCHO and CH_3CHO the values for $\emptyset_\lambda$ refer to the reactions

$$HCHO + h\nu \rightarrow H + HCO$$

$$CH_3CHO + h\nu \rightarrow CH_3 + HCO \quad .$$

4. SOLAR RADIATION

A treatment of solar radiation and its absorption from an air pollution point of view is given by Leighton (1961). The attenuation of solar radiation due to both gases and particles is considered, and a set of formulae suited for practical use is developed. Some data used by Leighton have been updated, but his method is still in use. See, for example, Demerjian and Shere (1975) and Calvert (1976). A description of Leighton's development which is modified somewhat for computer application and uses a more recent data base follows. Leighton's terminology is used.

4.1 Air mass and solar zenith angle

The air mass (m) is the length of path of the direct solar radiation through the atmosphere relative to the vertical path. The solar zenith angle (z) is the angle between the actual path and the vertical. For small z it is sufficient to use $m = 1/\cos z = \sec z$, but when the sun is closer to the horizon, corrections must be made due to refraction and the curvature of the earth. Leighton gives some corrected values for large angles ($z > 60°$). The corrected values, which are presented by Bemporad (1954), can be shown to follow quite closely a formula taking the curvature of the earth into account:

$$m = \sqrt{\alpha^2 \cos^2 z + 2\alpha + 1} - \alpha \cos z \qquad (4.1)$$

This formula is developed in Appendix C and has one parameter α which is the ratio between the radius of the earth and the height of the

atmosphere. In Table 3 some values for several α are shown together with the secant law values and the values recommended by Leighton.

Table 3. Air mass as a function of solar zenith angle

Solar zenith angle	60°	70°	80°	85°	88°	90°
Secant	2.00	2.92	5.76	11.47	28.7	∞
Bemporad (1954)	2.00	2.90	5.60	10.39	19.8	
This work, α=570	2.00	2.91	5.61	10.40	19.3	33.8
" α=600	2.00	2.91	5.61	10.44	19.6	34.7
" α=630	2.00	2.91	5.62	10.48	19.8	35.5

By a simple least squares method it was found that α≈630 gave the best fit for all five values between 60° and 88°, while α≈570 gave the best fit if z=88° was excluded. For the further work I chose α=600 (i.e., the height of the atmosphere 10.6 km). This value is not critical, however. If instead α=570 had been chosen, less than 0.1% change would have been obtained in the final photochemical rate constants.

The solar zenith angle is given by the declination (dec), the latitude (lat) and the local hour angle (lha):

$$\cos z = \cos \text{lat} \cdot \cos \text{dec} \cdot \cos \text{lha} + \sin \text{lat} \cdot \sin \text{dec} \quad (4.2)$$

For this work a simple expression for the declination as a function of month was chosen:

$$\text{dec} = 23.5 \sin (30t - 90) \quad (4.3)$$

where t is the month, such that t=6 means June 21, t=3 means March 21 etc. This formula gives the declination in degrees.

4.2 Molecular scattering and "particulate diffusion"

This development follows Leighton completely. The transmission due to molecular (Rayleigh) scattering as a function of air mass (and wavelength) is given by

$$\log_{10} T_{m\lambda} = -(S_{m\lambda})_{\circ} \frac{P}{P_{\circ}} m \qquad (4.4)$$

where the molecular scattering coefficient $(S_{m\lambda})_{\circ}$ is tabulated by Leighton, P is the actual pressure at ground level, $P_{\circ}$ the reference pressure and m is the air mass.

The term "particulate diffusion" is used to describe the combined effect of scattering (Mie), reflection, refraction and diffraction. Leighton uses an empirical equation proposed by Moon (1940) (λ in Ångstroms)

$$\log_{10} T_{p\lambda} = -(3.75 \cdot 10^{-3} \lambda^{-2} w + 3.5 \cdot 10^{-2} \lambda^{-0.75} d) m \qquad (4.5)$$

where the parameters w and d represent the concentration of water droplets and dust respectively. For urban atmospheres a good fit with observed transmission coefficients was found for w=2 and d=1.

4.3 Absorption by atmospheric ozone

The absorption by naturally occurring ozone occurs within two bands, the Huggins band (below 350 nm) and the Chappuis band (450-700 nm). In this work only the Huggins band between 290 and 350 nm

is considered. The reason for this is that no wavelengths shorter than 290 nm reach the earth's lower atmosphere, and for the photochemical reactions considered either the absorption coefficient or the quantum yield is zero for $\lambda > 440$ nm.

The transmissivity due to absorption by ozone is given by

$$\log_{10} T_{a\lambda} = - \alpha_\lambda [O_3] \, m \qquad (4.6)$$

where the absorption coefficients α_λ originally presented by Inn and Tanaka (1953) are tabulated by Leighton. The background concentration of ozone $[O_3]$ is expressed in mm STP. This is a function of latitude and season, and recent data are available in the CIAP reports (1975). Figure 2, taken from CIAP Monograph 3, gives the ozone content as a function of latitude and month. This graph has been computerized using a method outlined in Appendix D. The ozone content is expressed as a sine function of the month t:

$$[O_3] = a \sin (bt-c) + d \qquad (4.7)$$

where the coefficients a, b, c, d are latitude dependent (see Leighton, 1961, Figure 7).

While Leighton used the average value $[O_3] = 2.2$ mm STP the concentrations in Figure 2 are in the range 2.5-4.4 mm STP.

4.4 Ground level radiation

The solar flux at ground level or the actinic irradiance in the lower atmosphere is given by

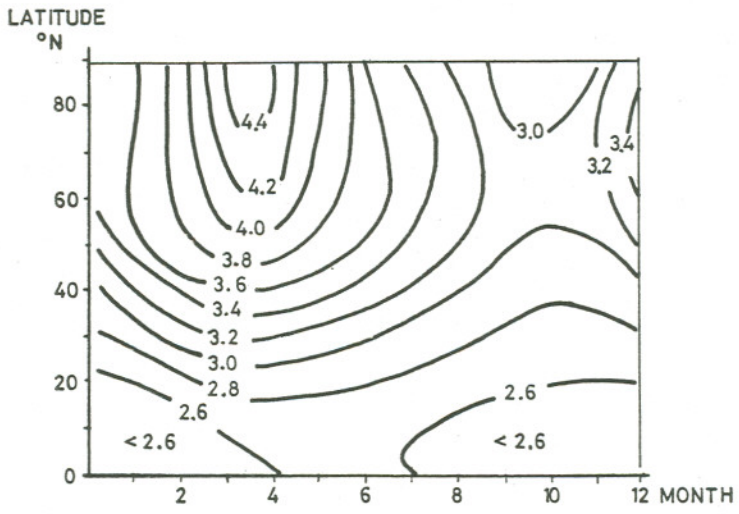

Figure 2. Natural ozone content (mm STP) as a function of month and latitude.
Source: CIAP Monograph 3 (1975).

$$J_\lambda = I_{o\lambda}\, T_{a\lambda}\, [T_{s\lambda} + g \cdot i\, (-T_{s\lambda}) \cos z] \qquad (4.8)$$

$$T_{s\lambda} = T_{m\lambda} \cdot T_{p\lambda} \qquad (4.9)$$

The flux J_λ has dimension photons $cm^{-2}s^{-1}10nm^{-1}$ and is a "volume flux", i.e., the flux of solar radiation incident on a spherical surface from all directions (Peterson and Demerjian, 1976).

The solar flux outside the atmosphere $I_{o\lambda}$ has been reviewed in the CIAP documents. The values recommended in the interval 290-440 nm are very close to those used by Leighton and originally published by Johnson (1954). The influence on the rate constants is less than 0.5%.

The coefficients g and i are related to the relative importance of direct and indirect (sky) radiation. Leighton recommends the values g=0.5 and i=2, hence

$$J_\lambda = I_{o\lambda}\, T_{a\lambda}\, [T_{s\lambda} + (1 - T_{s\lambda}) \cos z] \qquad (4.10)$$

Through the set of formulae given above J_λ can be calculated for any solar zenith angle, i.e. for any location on the northern hemisphere any time of the year.

Several simplifications have been made in obtaining this expression. The solar attenuation due to pollution, for example absorption by NO_2 and scattering by secondary aerosol, is neglected, and so is reflection from the earth's surface. Leighton claims that these two errors will partially cancel.

The effect of clouds is not considered; i.e., the day has to be clear for (4.9) and (4.10) to be valid.

5. SOLUTION METHODS

The calculation of time dependent concentrations from a photochemical reaction mechanism implies solving a set of non-linear first order differential equations.

If the mechanism is a part of an advection-diffusion model for an airshed, the problem also involves the solution of the continuity equation for the reactive species. This problem has been formulated and solved for the Los Angeles basin by Reynolds, Roth and Seinfeld (1973) using the 19 step mechanism mentioned in Chapter 2. Eschenroeder and Martinez (1972) used their photochemical mechanism together with a trajectory model for the Los Angeles area.

A simpler way of modeling "dispersion" is to consider one well-mixed cell in which the air is diluted by clean air at a constant rate (see for example Hesstvedt, 1975). This approach is also used for simulating smog chamber experiments in which dilution takes place.

Modeling of dispersion is beyond the scope of this report. The problem then reduces to solving a set of ordinary non-linear differential equation for given initial conditions. The solar dependent rate constants vary with time.

5.1 Stiff systems

The set of differential equations is "stiff"; i.e. there is a large distribution in characteristic times. Some reactions are very fast, and some are very slow. That can be seen from the rate constants given in Appendix 1. The second order rate constants vary between

10^{-6} and 10^{4} ppm^{-1} min^{-1}, about 10 orders of magnitude.

A standard integration code, for example of the Runge-Kutta or predictor-corrector type, must therefore use an extremely small step size in the integration. A simple solution method is to linearize the equations in the following way

$$\frac{dC_i}{dt} = P_i - Q_i C_i \qquad (5.1)$$

and assuming that the production rate P_i and the consumption "rate" Q_i are constant and independent of C_i over the integration interval. The equations are thus both linearized and decoupled and can be solved analytically. This method, combined with steady state approximations, is used by Hesstvedt, Hov and Isaksen (1976).

5.2 Steady state approximations

One way to reduce the stiffness of the system is to invoke the steady state assumption for the most reactive components. This implies assuming $dC_i/dt = 0$ for component i. This does not mean that the concentration does not vary with time, it means that the production rate equals the consumption rate at any instant. Mathematically to "steady-state" means replacing a differential equation by an algebraic equation.

If only a few components are steady-stated the algebraic equations may be linear, but when the number of steady-stated components increases, so does the non-linearity of the algebraic set of equations. Whether computing time will be saved or not, depends on whether the gain due to increased step-length and fewer differential

equations is larger than the loss due to solution of non-linear algebraic equations.

Also steady-stating introduces some error in the calculated concentrations. For example, as shown by Hecht, Liu and Whitney (1974), the components O, ROO· and RCO_3· may be steady-stated without significant loss in accuracy, while steady-stating of O_3 leads to large computational errors.

5.3 Gear's algorithm

There exist mathematical techniques for solving stiff differential equations. One such technique is described by Gear (1971) and is used in program "packages" for smog chamber simulations (see for example Hecht, Liu and Whitney (1974) or Whitten and Hogo (1976)). The codes based on Gear's method require a fairly large computer in terms of high-speed memory capacity, but they are relatively fast. Also the program packages are flexible in terms of adding or deleting reactions to the photochemical mechanism.

5.4 Choice of method

The solution method chosen for this work was a modified Hamming's predictor-corrector code with variable step-length (Hamming, 1962). The reasons for this choice were several. First, this code was available at Oregon Graduate Center. Second, the computer, a PRIME 300, had limited high-speed memory (64 K) and a FORTRAN compiler which required some changes in programs written for IBM or CDC computers. For the limited time available for this work I therefore chose a program at

hand, and reasonable execution times were obtained by applying the steady state assumption to the organic and inorganic radicals. The accuracy which may be lost by this approach is discussed in chapter 6.

In Appendix E the computer program is shown. The main program sets the initial conditions and parameters used in the computation. Subroutine FCT generates the concentration of the components which are steady-stated and calculates the derivatives of the components which are computed by the predictor-corrector code DHPCG. DHPCG is not shown in Appendix E. Subroutine PHOTO generates the photolytic rate constants, and subroutine TOZONE generates the background ozone content. Subroutine OUTP prints out the results.

6. RESULTS AND DISCUSSION

6.1 Photolytic rate constants

6.1.1 Validation of the computations

The photolytic rate constants for the five reactions described in paragraphs 2.1.1 - 2.1.5

$$NO_2 + h\nu \rightarrow NO + O(^3P)$$

$$HNO_2 + h\nu \rightarrow NO + OH$$

$$H_2O_2 + h\nu \rightarrow 2OH$$

$$HCHO + h\nu \rightarrow H + HCO$$

$$CH_3CHO + h\nu \rightarrow CH_3 + HCO$$

were computed as a function of solar zenith angle. These are the reactions used in the Hecht, Seinfeld and Dodge model (1974). The computer program was checked by comparing with the results given by Demerjian and Schere (1975) for two solar zenith angles, 0° and 80°. For this comparison the background ozone concentration was set equal to 2.2 mm STP, the value used by Leighton (1961). The comparison is shown in Table 4. There are slight deviations in the results, especially for the photodissociation of HNO_2, but the deviation is probably not large enough to suspect that the computer program contains specific errors.

Table 4. Comparison of photolytic rate constants (min^{-1}).

Solar zenith angle	0°	80°
$NO_2 + h\nu \rightarrow NO + O(3p)$		
Demerjian and Schere	0.600	0.107
This work	0.622	0.111
$HNO_2 + h\nu \rightarrow NO + OH$		
Demerjian and Schere	$0.350 \cdot 10^{-1}$	$0.598 \cdot 10^{-2}$
This work	$0.386 \cdot 10^{-1}$	$0.664 \cdot 10^{-2}$
$H_2O_2 + h\nu \rightarrow 2OH$		
Demerjian and Schere	$0.194 \cdot 10^{-2}$	$0.240 \cdot 10^{-3}$
This work	$0.193 \cdot 10^{-2}$	$0.238 \cdot 10^{-3}$
$HCHO + h\nu \rightarrow H + HCO$		
Demerjian and Schere	$0.271 \cdot 10^{-2}$	$0.258 \cdot 10^{-3}$
This work	$0.267 \cdot 10^{-2}$	$0.253 \cdot 10^{-3}$
$CH_3CHO + h\nu \rightarrow CH_3 + HCO$		
Demerjian and Schere	$0.606 \cdot 10^{-3}$	$0.318 \cdot 10^{-4}$
This work	$0.588 \cdot 10^{-3}$	$0.283 \cdot 10^{-4}$

6.1.2 The dependence of the photolytic rate constants on season and latitude.

The diurnal variation of the rate constant for

$NO_2 + h\nu \rightarrow NO + O(^3P)$

is shown in Figure 3 for June 21st for four cities in the northern

hemisphere, Los Angeles, California (34°N), Portland, Oregon (45.5°N), Rotterdam, The Netherlands (52°N) and Oslo, Norway (60°N). The figures show that in the summer the rate constant is higher in the northern latitudes during the early morning and late afternoon. This is due to the early sunrise and late sunset in the high latitudes during the summer. Around noon, however, the rate constant is higher in the low latitudes.

Figure 4 shows the diurnal variation for October 21st. On this date, which is later than the equinox, the lower latitudes have higher rate constants all through the day.

Figures 5 and 6 show the diurnal variation for the same two dates and four cities of the rate constant of the reaction

$$HCHO + h\nu \rightarrow H + HCO$$

The trends are very much the same as for the dissociation of NO_2, except that the relative differences due to latitude are larger for dissociation of HCHO than for NO_2. The reason is that NO_2 dissociates by radiation up to 440 nm while HCHO does not dissociate above 360 nm. When the solar zenith angle increases, the high energy solar radiation is attenuated more than the low energy radiation. This effect is even more pronounced for the reaction

$$O_3 + h\nu \rightarrow O_2 + O(^1D)$$

which takes place for $\lambda \leqslant 310$ μm (see Demerjian and Schere, 1975).

The seasonal dependency for photodissociation of NO_2 is shown in Figures 7-9 for the same four latitudes as before and for three local hours, 1200 (noon), 0900 and 0600. The rate constant is set equal to zero if the solar zenith angle is

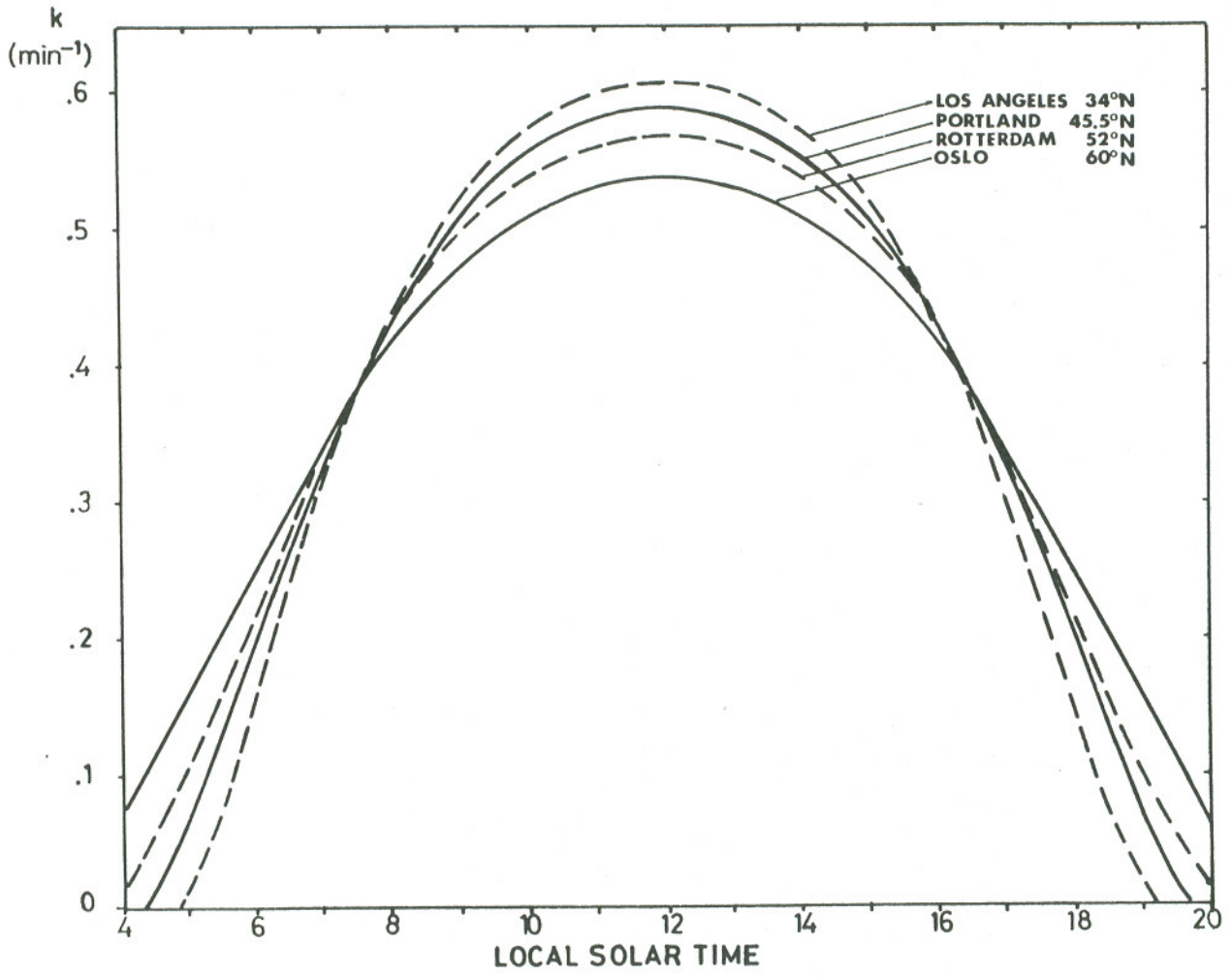

Figure 3. Rate constant for $NO_2 + h\nu \rightarrow NO + O(^3P)$ as a function of local solar time on June 21st for four latitudes.

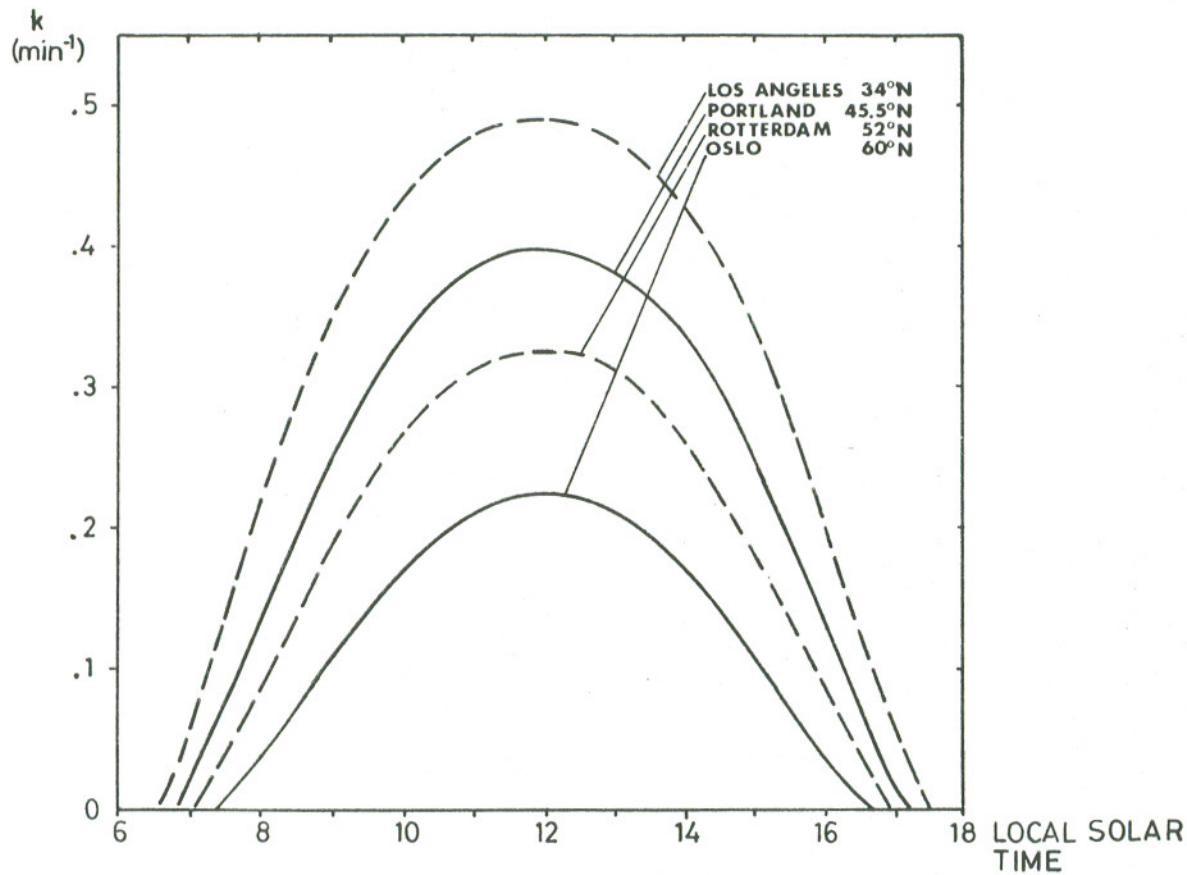

Figure 4. Rate constant for $NO_2 + h\nu \rightarrow NO + O(^3P)$ as a function of local solar time on October 21st for four latitudes.

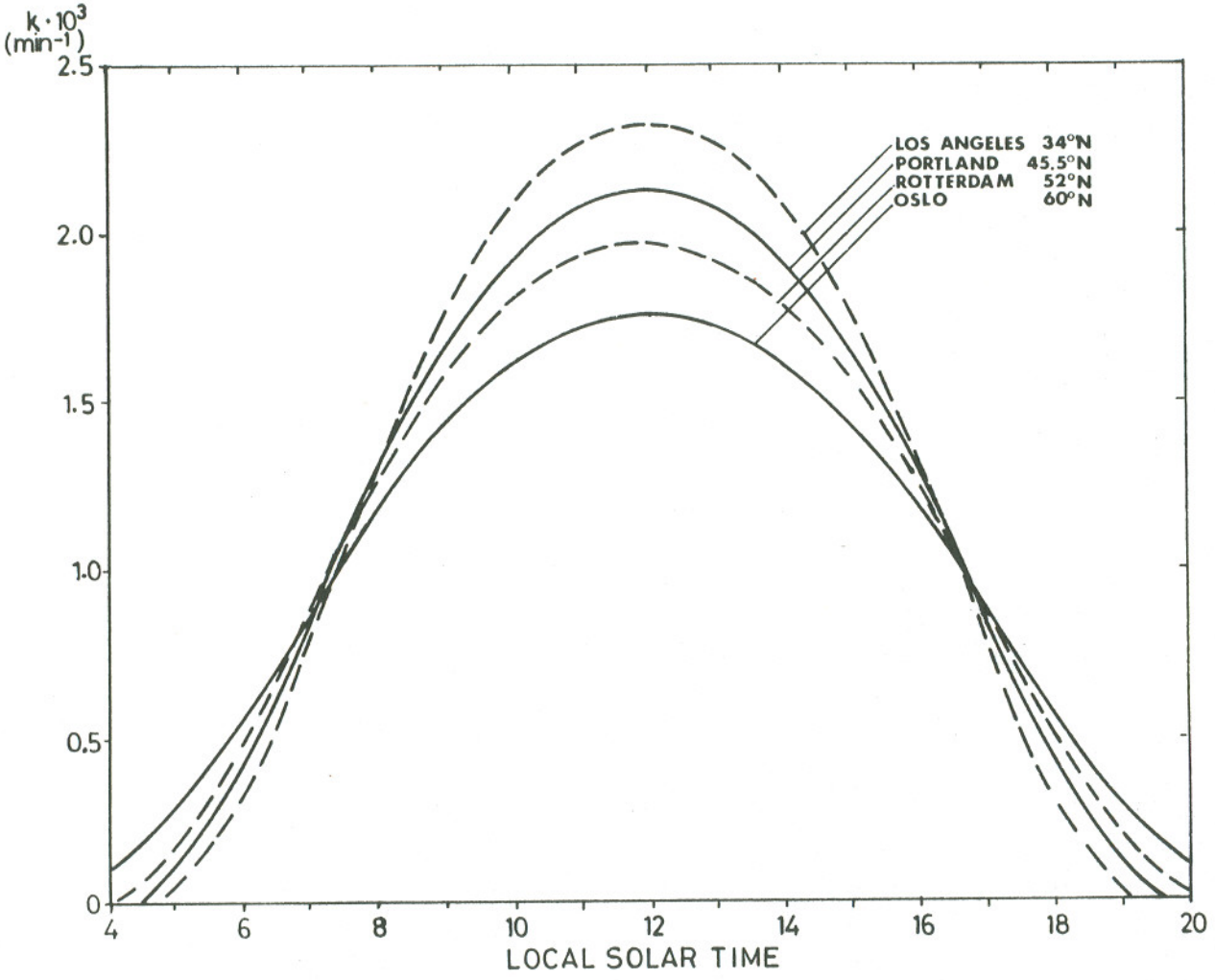

Figure 5. Rate constant for HCHO + hν → H + HCO as a function of local solar time on June 21st for four latitudes.

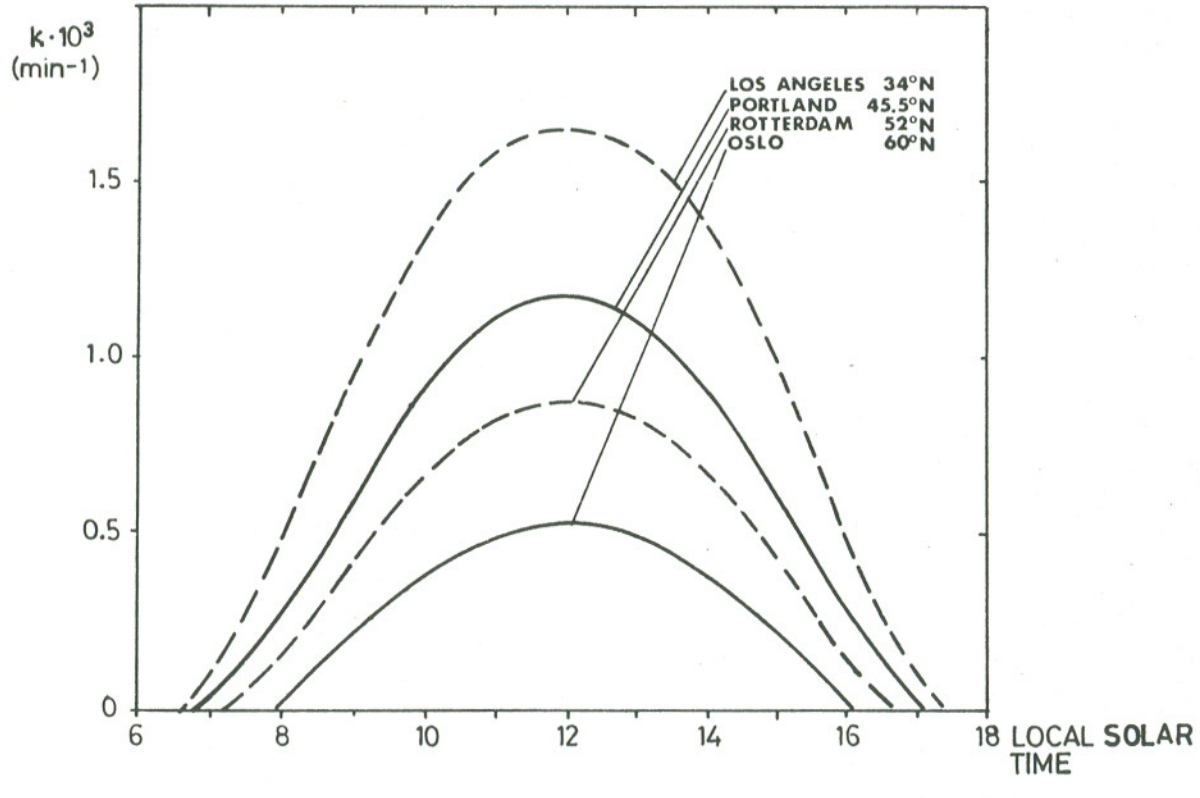

Figure 6. Rate constant for HCHO + hν → H + HCO as a function of local solar time on October 21st for four latitudes.

larger than or equal to 90°. At noon the low latitudes have a higher rate constant all through the year, as shown in Figure 7. The same is the case at 0900 (Figure 8), but in the summer the curves for the four latitudes are quite close. At local time 0600 there is only sunshine between March 21 and September 21 and the high latitudes have higher rate constants than the low latitudes. Indeed, no place on earth has a higher rate constant at local time 0600 any time of the year than the north pole.

In Appendix F the seasonal and latitude dependencies for all five photolytic reactions are given for the 21st of each month and for 10° latitude intervals from the equator to the north pole. Three local hours are considered: 1200, 0900 and 0600. The trends are essentially the same as shown in Figures 3-9.

6.2 Simulation of photochemical smog

6.2.1 Validation of the solution method

The solution method was checked by choosing a run described by Hecht, Seinfeld and Dodge (1974), the EPA run 325, and comparing the output for the same rate constants and the same initial conditions. Four species were assumed by Hecht, Seinfeld and Dodge to be in pseudosteady state: O, NO_3, OH and RO. The result of the comparison is shown in Figure 10 giving the time dependencies for propylene, NO, NO_2, O_3 and PAN (more correctly peroxyacylnitrates) for the EPA run 325. The ozone values computed in this work were about 10% higher than those computed by Hecht, Seinfeld and Dodge (1974). The difference may to some extent be due to the solution method, or it may be

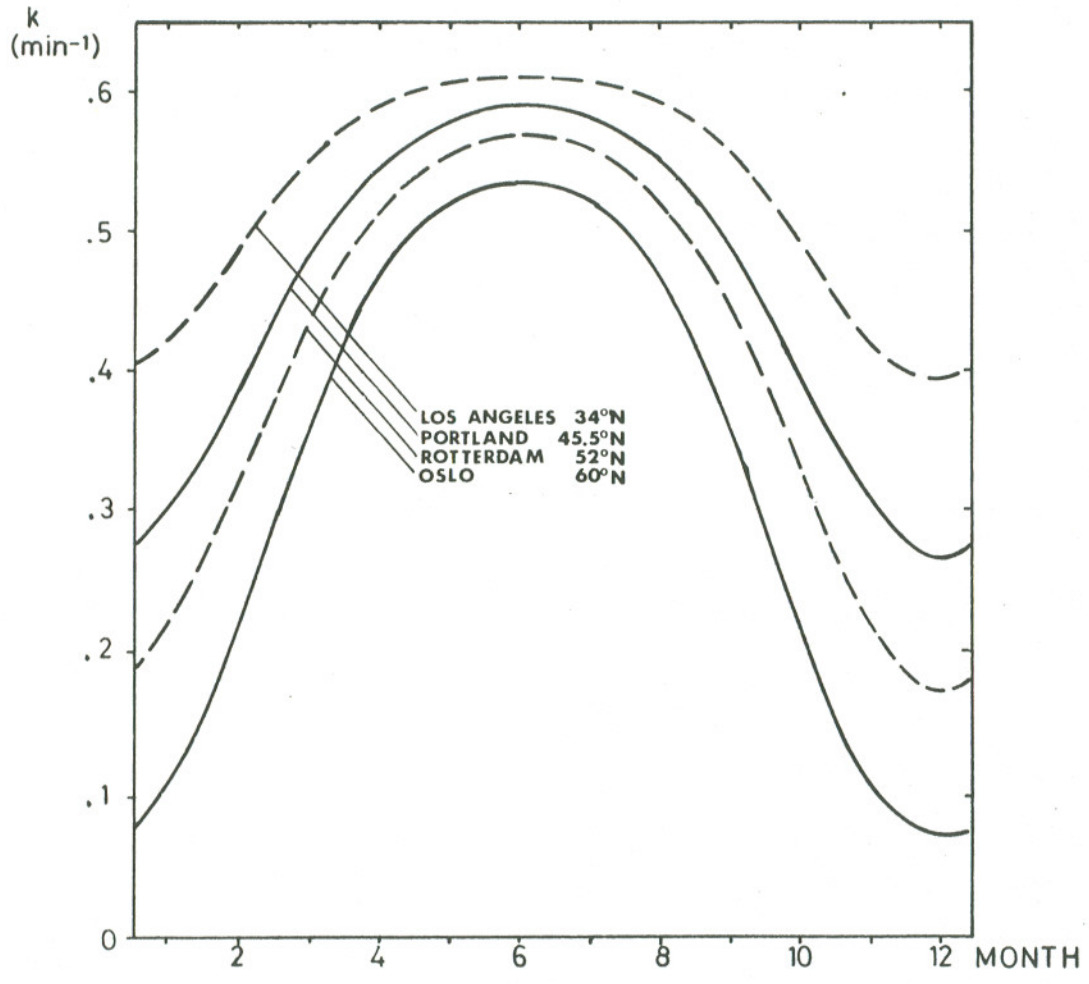

Figure 7. Rate constant for $NO_2 + h\nu \rightarrow NO + O(^3P)$ as a function of month at local solar time 12.00 (noon) for four latitudes.

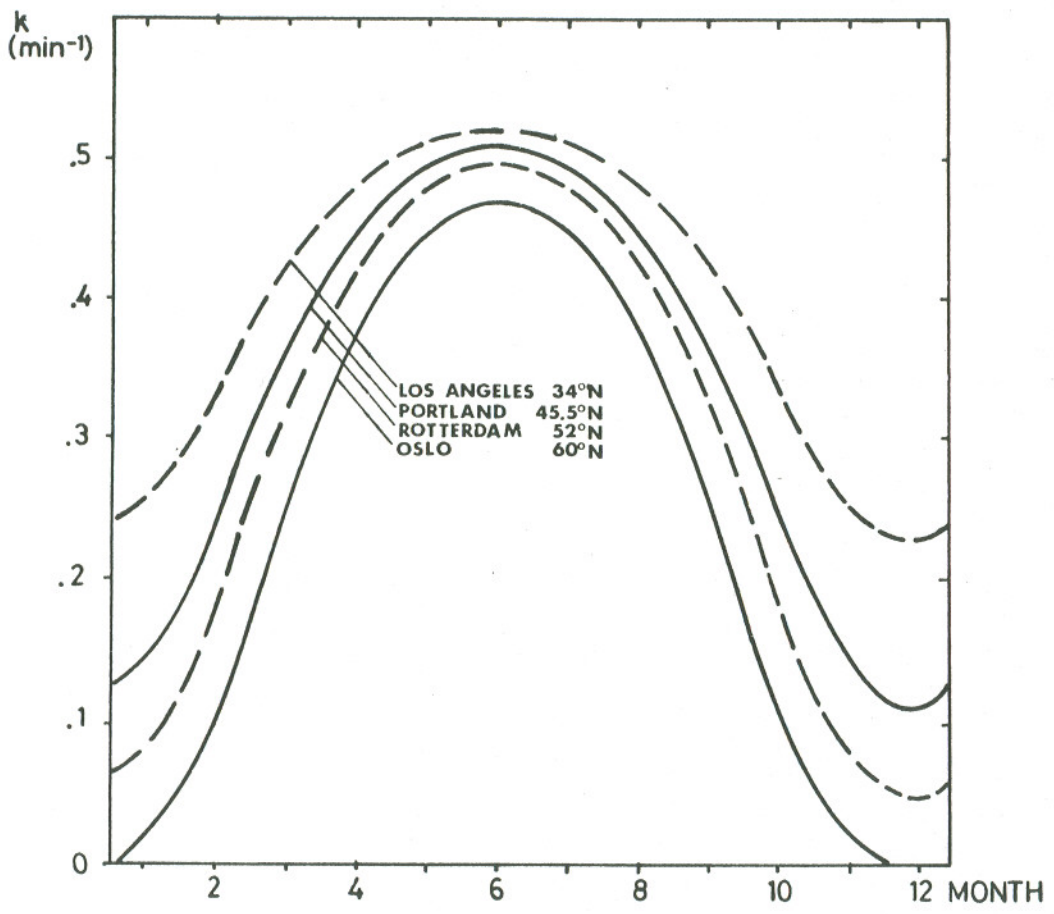

Figure 8. Rate constant for $NO_2 + h\nu \rightarrow NO + O(^3P)$ as a function of month at local solar time 0900 for four latitudes.

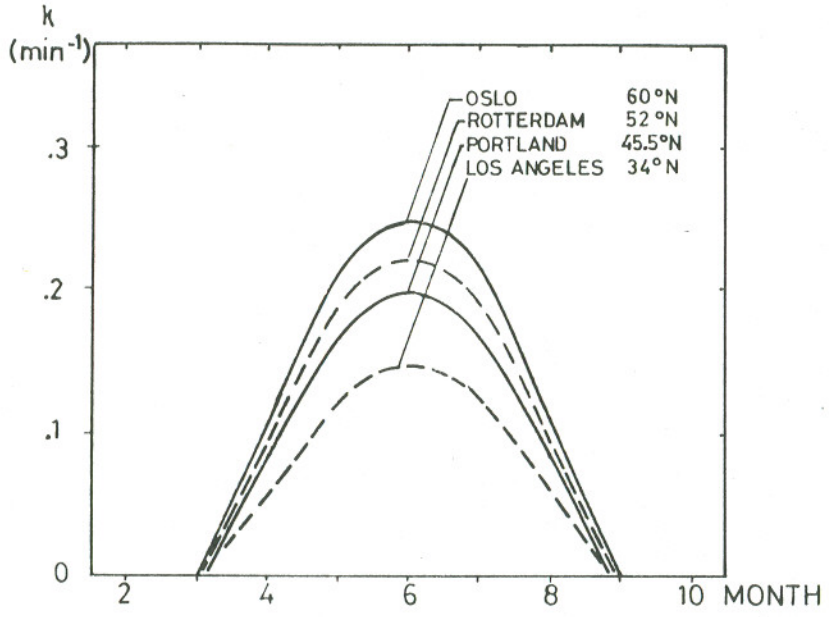

Figure 9. Rate constant for $NO_2 + h\nu \rightarrow NO + O(^3P)$ as a function of month at local solar time 0600 for four latitudes.

be due to differences in water vapor concentration. In this work $[H_2O]$ = 15000 ppm was used, which corresponds approximately to 50% relative humidity at 25°C. The results were still, however, within the range of the experimental results.

The computing time for the Hamming's predictor-corrector solution method was very long: 180 minutes real time took about 60 minutes on the PRIME computer; the average step length was about 0.1 seconds. An attempt was made to speed up the efficiency of the solution method. In a sensitivity study Hecht, Liu and Whitney (1974) found that reactions 4, 6, 12, 13, 38 and 39 were the least important ones, and they recommended deleting these reactions from the scheme. When that was done it was much easier to apply the steady state assumption to the radicals ROO and RCO_3, the peroxyalkyl and peroxyacyl radicals. As a result, the computing time was reduced by a factor of 7, and the concentrations of the major species, NO, NO_2, propylene, ozone and PAN changed less than 1%, i.e. the run was essentially indistinguishable from the previous one.

In order to further speed up the calculation, the radical HO_2 was steady-stated. The computing time was reduced by a factor of 3, and the result is shown in Figure 10. The ozone and PAN concentrations were 5-10% larger than in the previous run. Apparently the steady state assumption for HO_2 introduced an error in the computations.

The influence on the NO_2 peak is shown in Table 5. The NO_2 peak was ca. 10% higher than predicted by Hecht, Seinfeld and Dodge (1974), but was not influenced by the steady state assumption for HO_2.

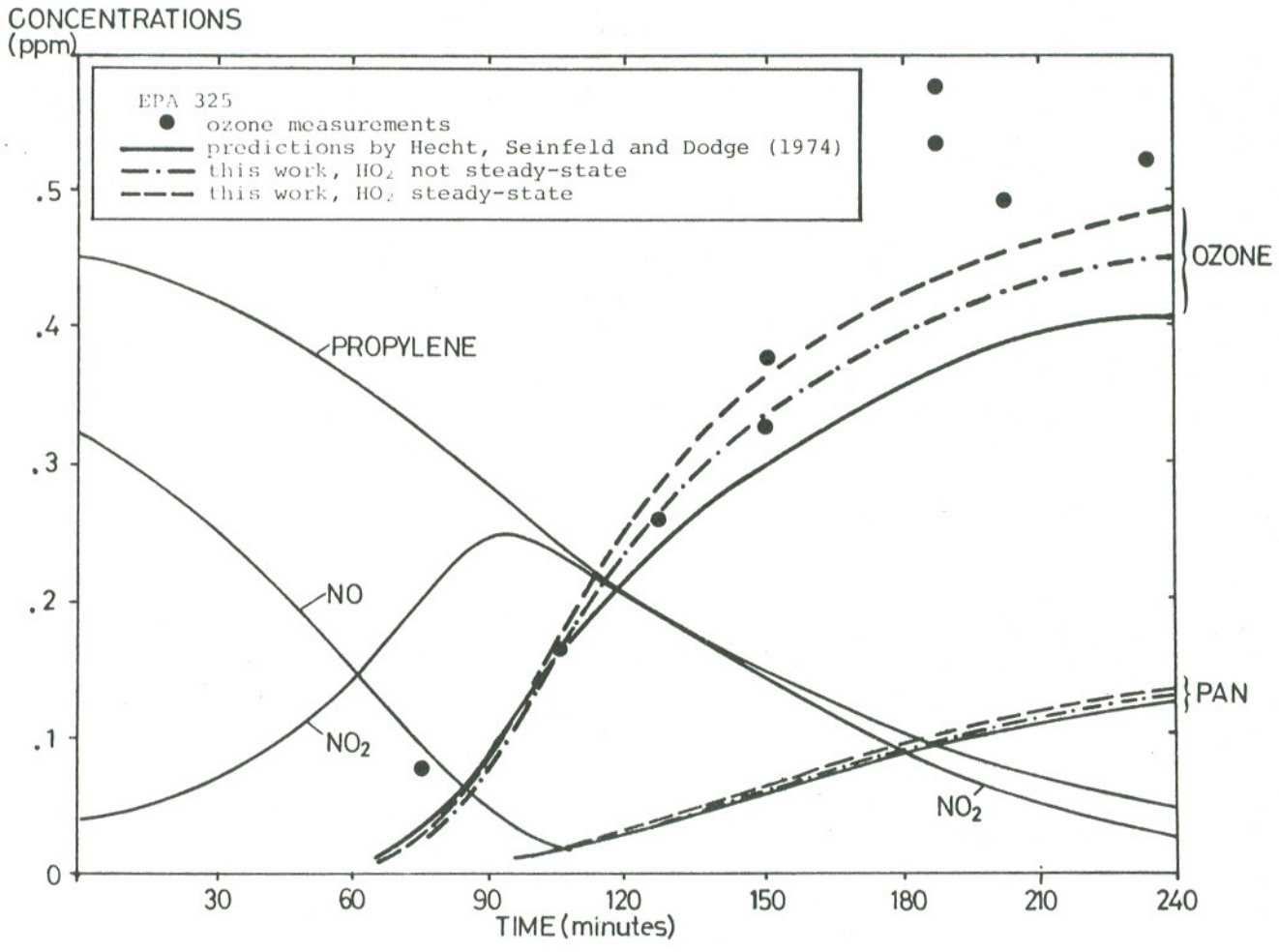

Figure 10. Comparison of predicted concentrations for EPA run 325.

Table 5. Influence of solution method on NO_2 peak.

	Time to NO_2 peak (minutes)	Magnitude of NO_2 peak (ppm)
Hecht, Seinfeld and Dodge	90-95	0.25
This work, HO_2 not steady-state	95	0.27
This work, HO_2 steady-state	95	0.27

For the rest of this work HO_2 was steady-stated. The reason is that it is not of interest here to predict accurate ozone or peroxyacyl-nitrate concentrations per se; the object of this work is to examine differences due to season and latitude. It is believed that the bias introduced by the HO_2 steady state assumption does not alter the relative differences due to latitude and season.

6.2.2 Specification of the runs.

It is well-known that the ozone levels obtained from irradiation of mixtures of hydrocarbons and nitrogen oxides are highly dependent on both the absolute initial concentrations and the ratio between hydrocarbons and nitrogen oxides. This has been shown both experimentally and theoretically and can, for example, be seen from Figure 11, taken from Hecht, Seinfeld and Dodge (1974). This graph is based on hydrocarbon mixtures of 25% propylene and 75% n-butane and a fixed NO_2 concentration of 0.1 ppm. Point A of Figure 11 represents the approximate composition of the Los Angeles atmosphere in 1969.

The binary mixture of propylene and n-butane was used to represent the complex mixture of hydrocarbons found in urban atmospheres.

This makes sense because propylene is more reactive than an average urban hydrocarbon mixture while n-butane is less reactive.

For this study an initial mixture representing point B on Figure 11 was chosen. The concentrations are lower than A because the Los Angeles air is more polluted than most urban areas. Point B is chosen on the ozone "ridge," i.e. a reduction of either NO_x or hydrocarbons will reduce the ozone concentration.

The initial mixture consisted of

0.15 ppm NO

0.10 ppm NO_2

0.15 ppm propylene

0.45 ppm n-butane

Because no aromatics or carbon monoxide was present, the reaction mechanism could be further simplified by deleting reactions 19, 25 and 26.

The rate constant for reaction 29, photolysis of aldehydes, was computed by weighting the formaldehyde and acetaldehyde photolysis rate constants by the coefficient β, which is the fraction of aldehydes which are not formaldehyde.

$$k_{29} = (1-\beta)\ k_{HCHO} + \beta \cdot k_{CH_3CHO}$$

Acetaldehyde was thus used to represent all higher aldehydes. The value of β for the n-butane/propylene/NO_x system was estimated by Hecht, Seinfeld and Dodge (1974) to be equal to 0.63. The parameter α is equal to 0.5 for propylene, (see paragraph 2.9).

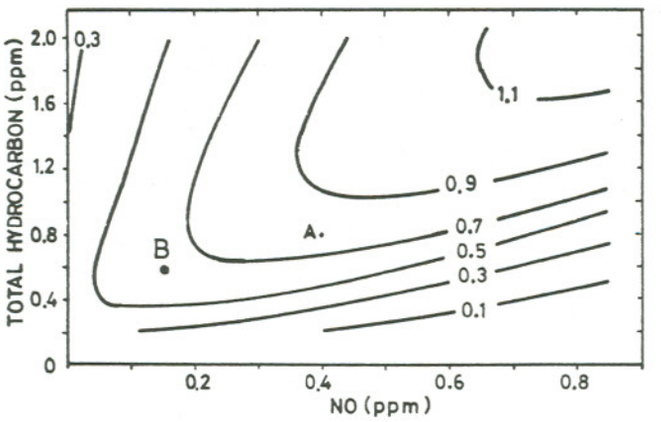

Figure 11. Isopleths of predicted maximum ozone concentrations during 8 hours irradiation of various mixtures of propylene, n-butane and NO. (Initial NO_2 concentration equal to 0.1 ppm). Source: Hecht, Seinfeld and Dodge (1974).

The specified mixture was irradiated at different latitudes and seasons. In order to evaluate the photochemical smog potential, a relatively short irradiation time was chosen, namely 3 hours. The reason for this is that the "closed, well-mixed cell" concept which a simulation like this implies, becomes increasingly unrealistic in the real atmosphere when the irradiation time increases. Two irradiation time intervals were chosen, 0900-1200 and 0600-0900 local time. The photolytic rate constants were updated every minute during the irradiation.

6.2.3 The dependency on latitude and season of the formation of ozone, peroxyacylnitrates and aldehydes.

Figure 12 shows the ozone concentration after 3 hours of irradiation at local time 0900-1200 for the months June-December and the latitudes between 30°N and the North Pole. The latitudes between the equator and 30°N were not examined because they would show essentially the same results as 30°N except for the seasonal shift due to the zenith position of the sun at 23.5°N at the summer solstice. This can be seen from the rate constants given in Appendix E.

The months between January and June were not examined either because of the near symmetry around the summer solstice. This symmetry is not complete due to the seasonal variation in the background ozone concentration (see Figure 2). However this effect is rather small. While the ozone concentration predicted at 70°N on August 21 was 154 ppb, the concentration on April 21 was 141 ppb, i.e. 8.4% lower. At lower latitudes the difference is smaller, for example at 30°N the concentration on April 21 was 3.1% lower than that of August 21.

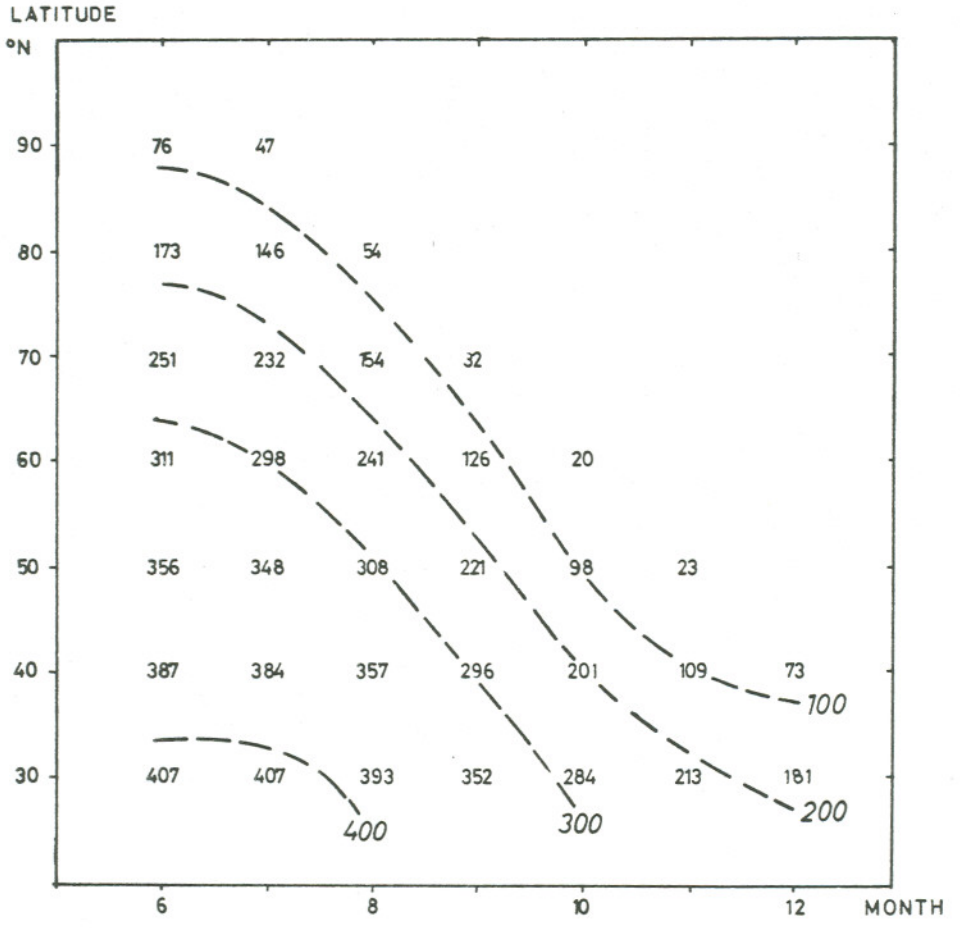

Figure 12. Predicted ozone concentrations (ppb) after 3 hours irradiation of 0.15 ppm NO, 0.10 ppm NO_2, 0.15 ppm propylene and 0.45 ppm n-butane at local solar time 0900-1200.

In Figure 12 isopleths showing constant ozone concentrations are indicated. These curves divide Figure 12 into areas with comparable photochemical smog potential due to radiation. It is evident that in the summer there is a potential for photochemical smog rather far north; at summer solstice the ozone concentration at 60°N was about 78% of that at 34°N. In the fall (and spring) the area of photochemical smog potential narrows considerably; at equinox the ozone concentration at 60°N was only 39% of that at 34°N.

If the irradiation period 0600-0900 local time is considered, the potential at northern latitudes is even more pronounced. This can be seen from Figure 13. Here only the months June-September are shown; later in the year the ozone formation was negligible.

One may counter that Figure 13 is irrelevant because the activity normally associated with photochemical smog, automobile traffic, is rather low at 6 a.m. However, if there are significant stationary sources in an area emitting hydrocarbons and nitrogen oxides, there may be some interest in evaluating the early morning smog potential. In some areas stationary sources contribute significantly to the photochemical smog formation. This has, in fact, been reported from The Netherlands (Guicherit, 1973).

From Figures 12 and 13 it can be seen that except for latitudes north of 70°N the photochemical smog potential during the period 0600-0900 is equal to or less than half of that during the period 0900-1200.

In Figures 14 and 15 the concentration of peroxyacylnitrates

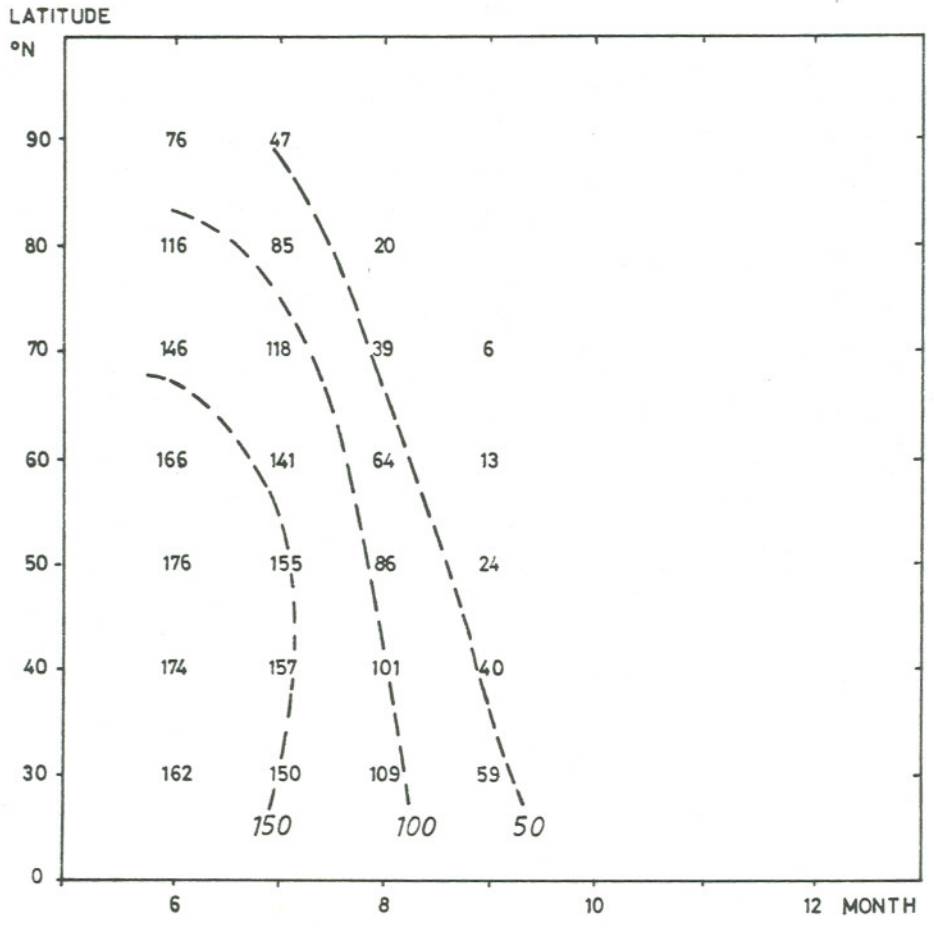

Figure 13. Predicted ozone concentrations (ppb) after 3 hours irradiation of 0.15 ppm NO, 0.10 ppm NO_2, 0.15 ppm propylene and 0.45 ppm n-butane at local solar time 0600-0900.

is plotted as a function of latitude and month for the irradiation periods 0900-1200 and 0600-0900. The concentration levels of peroxyacyl-nitrates were approximately one order of magnitude lower than those of ozone. The variation with latitude and season was generally the same as that of ozone.

In Figures 16 and 17 the concentration of aldehydes is plotted as a function of latitude and month for the two irradiation periods. The aldehyde concentration levels were of the same order of magnitude as those of ozone, but the relative differences were somewhat smaller. This must be due to the photolytic dissociation of aldehydes and the reaction with OH, which reduces the aldehyde build-up when the radiation is strong.

Generally there was good correlation between the levels of ozone, peroxyacylnitrates and aldehydes. This has been reported earlier by other investigators (see for example Hesstvedt, Hov and Isaksen, 1976).

The runs were further examined by looking at the time necessary to obtain maximum NO_2 concentration as a function of month and latitude. The results are shown in Figure 18. The notation ">180" indicates that the NO_2 maximum was not obtained during the 3 hours irradiation. The isopleths in Figure 16 correspond closely with those for ozone and peroxyacylnitrates. This confirms that the time necessary for NO_2 to reach its maximum concentration is an important variable in the photochemical cycle, as earlier pointed out by others (Hecht, Roth and Seinfeld, 1973). It can be seen from Figure 10 that

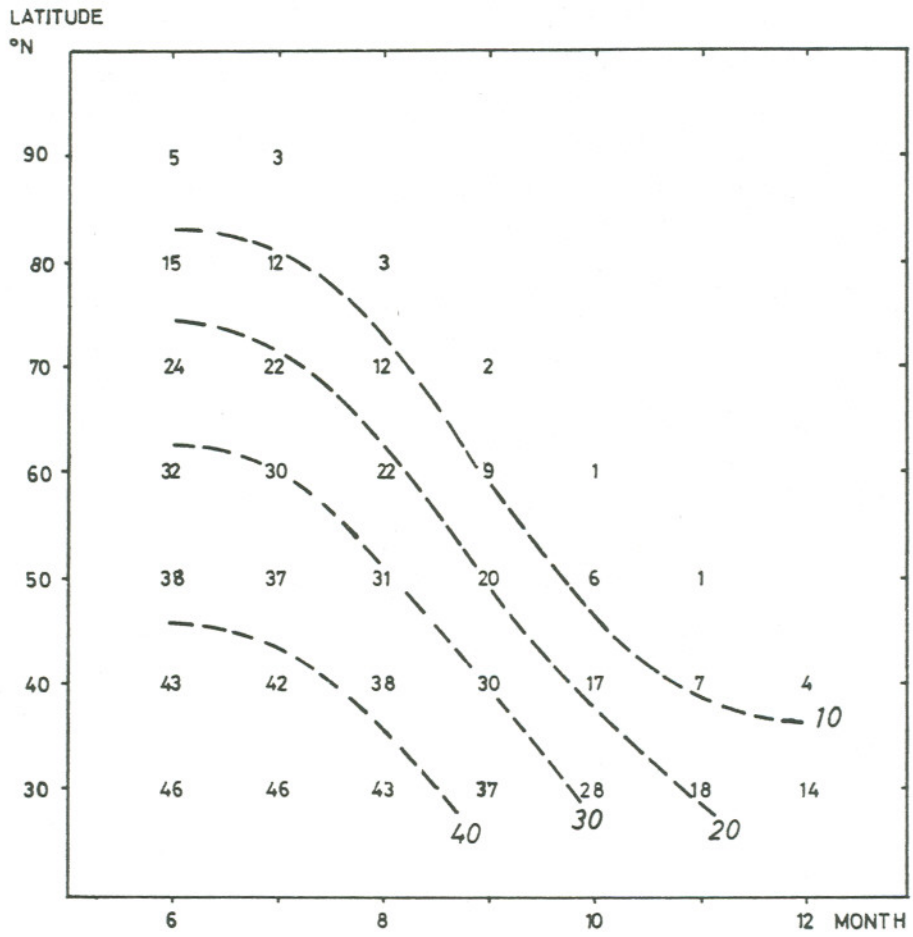

Figure 14. Predicted concentrations of peroxyacylnitrates (ppb) after 3 hours irradiation of 0.15 ppm NO, 0.10 ppm NO_2, 0.15 ppm propylene and 0.45 ppm n-butane at local solar time 0900-1200.

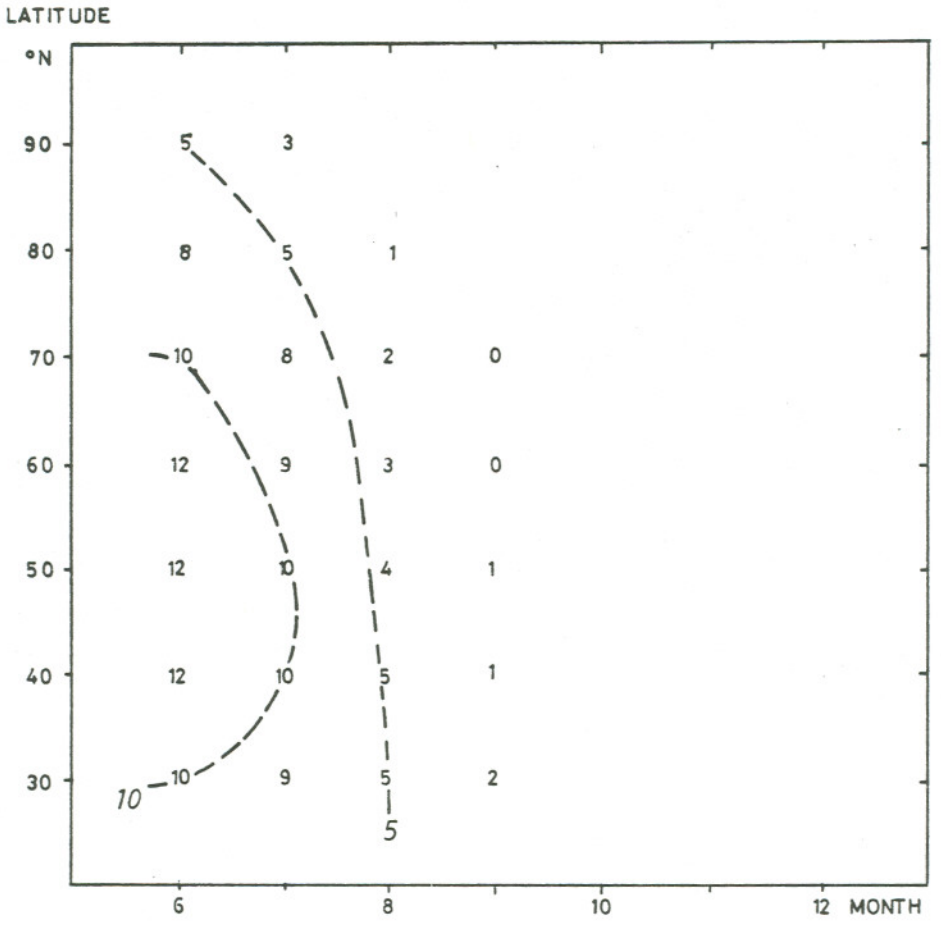

Figure 15. Predicted concentrations of peroxyacylnitrates (ppb) after 3 hours irradiation of 0.15 ppm NO, 0.10 ppm NO_2, 0.15 ppm propylene and 0.45 ppm n-butane at local solar time 0600-0900.

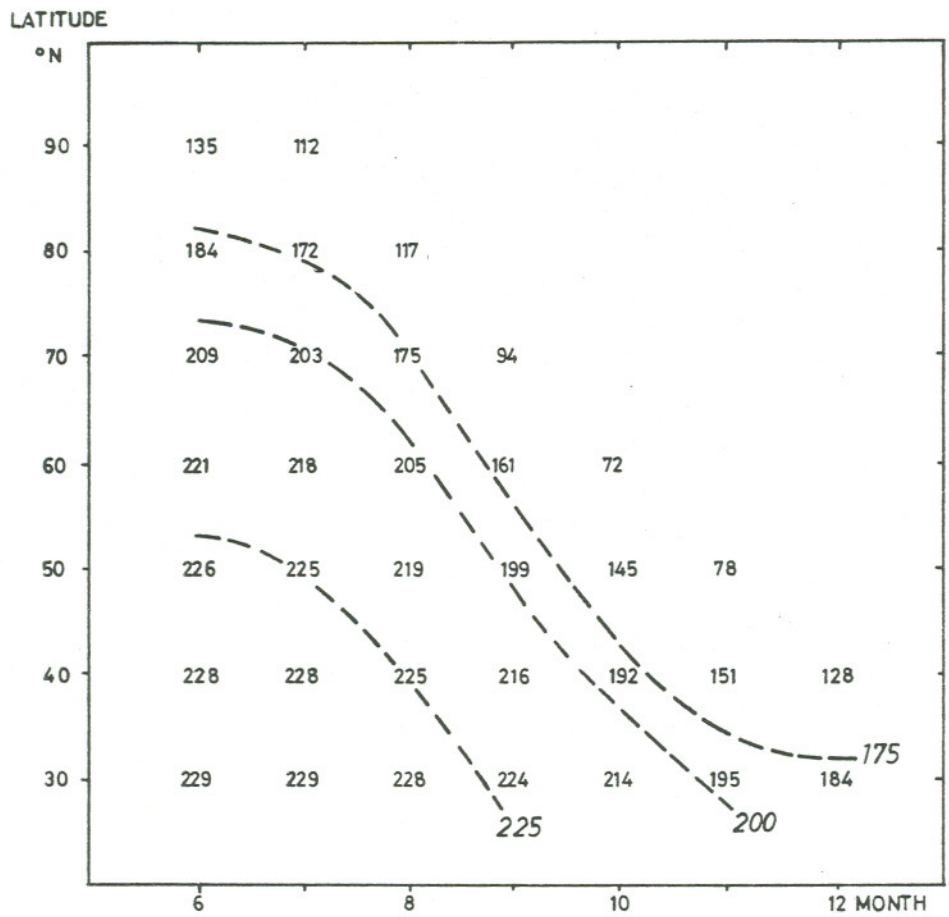

Figure 16. Predicted concentrations of aldehydes (ppb) after 3 hours irradiation of 0.15 ppm NO, 0.10 ppm NO_2, 0.15 ppm propylene and 0.45 ppm n-butane at local solar time 0900-1200.

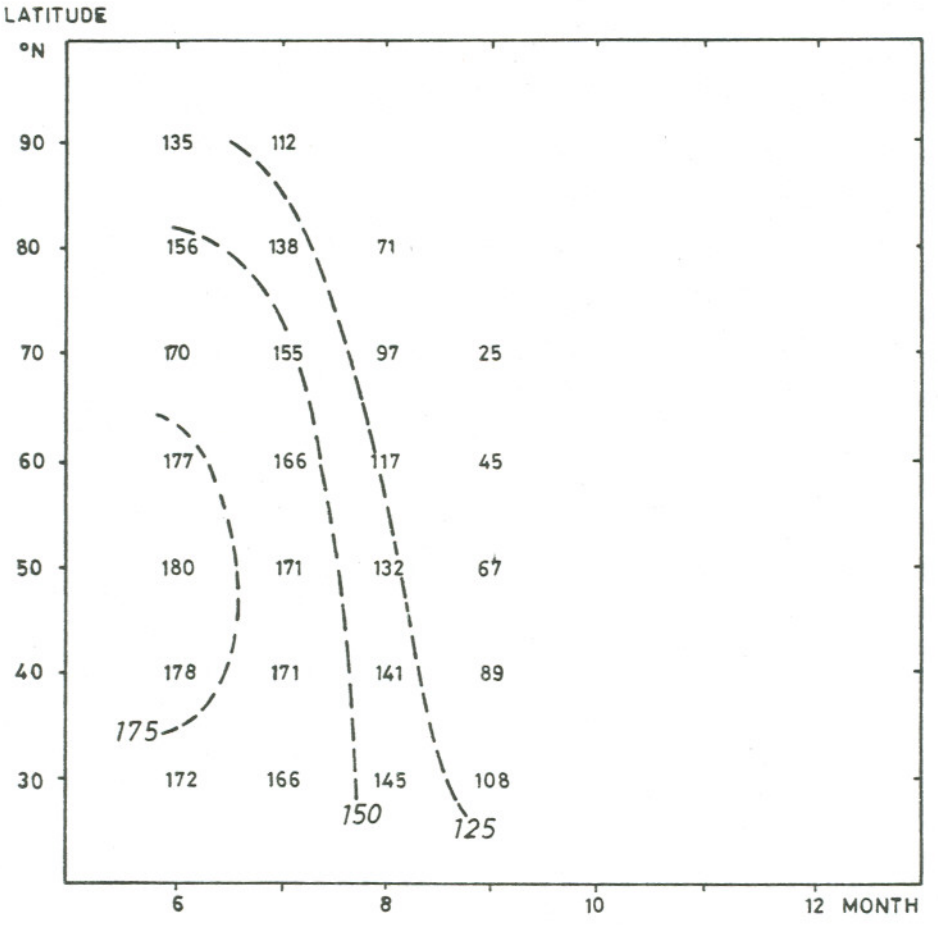

Figure 17. Predicted concentrations of aldehydes (ppb) after 3 hours irradiation of 0.15 ppm NO, 0.10 ppm NO_2, 0.15 ppm propylene and 0.45 ppm n-butane at local solar time 0600-0900.

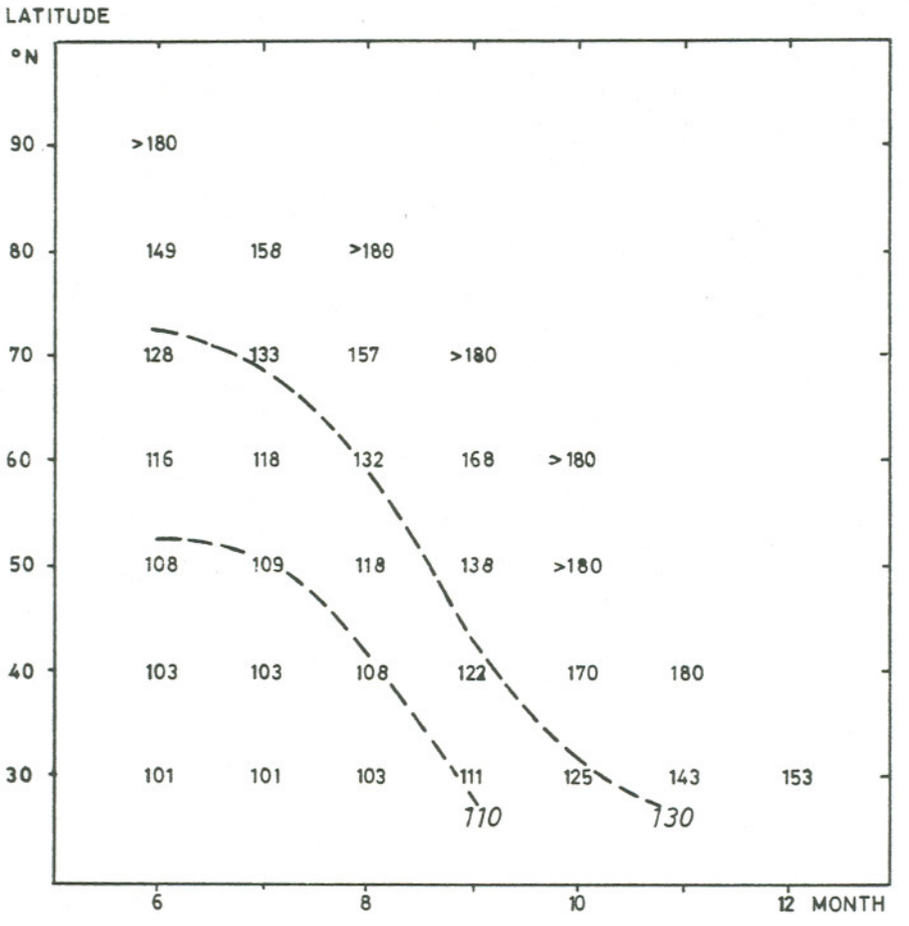

Figure 18. Predicted times to reach maximum NO_2 concentration (minutes) at 3 hours irradiation of 0.15 ppm NO, 0.10 ppm NO_2, 0.15 ppm propylene and 0.45 ppm n-butane at local solar time 0900-1200.

the ozone concentration increases rapidly when NO_2 peaks. This can also be seen from reactions 1 and 2 in the photochemical cycle (paragraph 2.2), which are the main reactions for ozone production. By neglecting other reactions involving $O(^3P)$ and O_3 consumption and applying the steady state assumption to $O(^3P)$, we get

$$\frac{d[O_3]}{dt} = k_1 [NO_2] \qquad (6.1)$$

i.e., assuming k_1 approximately constant the ozone curve is steepest when NO_2 peaks.

Figure 19 gives the magnitude of the NO_2 peak for different latitudes and months. In this figure the number after the > sign is the NO_2 concentration after 3 hours irradiation for the cases in which the NO_2 maximum was not reached. Figure 19 shows that the magnitude of the NO_2 peak is not very much influenced by changes in latitude and season, and the value decreases slightly when the solar flux increases. This can be explained by an approximate equation for the NO_2 formation

$$\frac{d[NO_2]}{dt} = [NO] \Sigma k_i[R_i] - k_1[NO_2] \qquad (6.2)$$

in which k_i and $[R_i]$ represent all reactions converting NO to NO_2:

$$R_i + NO \xrightarrow{k_i} R_j + NO_2$$

and where R_i includes ROO , RCO_3 , HO_2 , NO_3 and ozone. The NO_2 maximum can then be expressed as

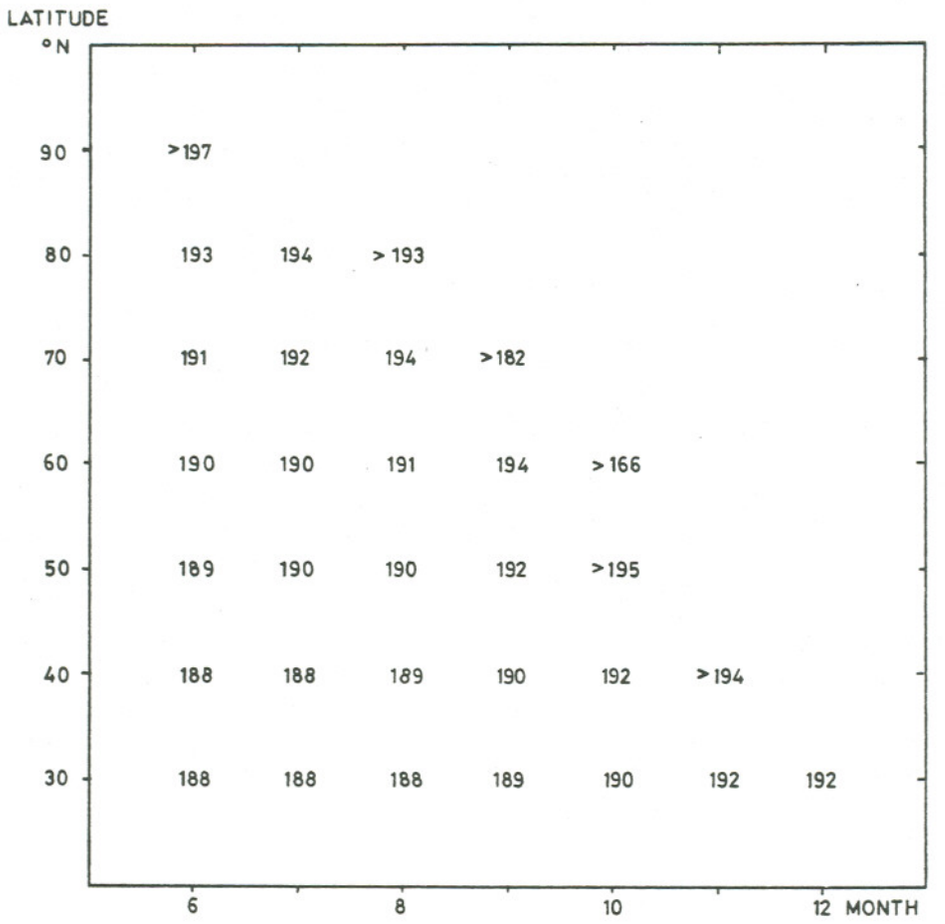

Figure 19. Predicted maximum NO_2 concentrations (ppb) during 3 hours irradiation of 0.15 ppm NO, 0.10 ppm NO_2, 0.15 ppm propylene and 0.45 ppm n-butane at local solar time 0900-1200.

$$[NO_2]_{max} = \frac{[NO] \Sigma k_i [R_i]}{k_1}$$

When the solar flux increases, so does k_1, but the concentration of radicals $[R_i]$ increases at the same time due to a more rapid hydrocarbon consumption. The net result was a slight decrease in the maximum NO_2 concentration.

6.3 Limitations of the study

The criteria generally used to conclude whether a certain location has a photochemical oxidant problem or not is the U.S. National Air Quality Standard for ozone, 0.08 ppm, an hourly average which may be exceeded once per year. The ozone concentrations given in this report should not be compared directly with this standard because the computations are based on assumptions which do not pertain to a specific airshed. The concentrations given here should be considered as relative, not absolute.

Even if solar radiation is the driving force of photochemical smog formation, other conditions must be met for photochemical smog to develop in an actual airshed. First, the emissions of hydrocarbons and nitrogen oxides must be above some threshold values, the magnitudes of which are not easily specified in practice. Second, the mixing ratio between hydrocarbons and nitrogen oxides must be within certain limits (see Figure 11). Third, the residence time of the precursors in the airshed must be long enough for the reactions to proceed before the pollutants are completely dispersed.

Therefore to evaluate the photochemical smog potential in an actual airshed an advection/diffusion model - in which an appropriate photochemical reaction mechanism is included - should be used. In such a model both the meteorological factors and the emission pattern can be taken into account. There are still, however, problems regarding validation of the results from the photochemical airshed models.

In this work one initial mixture was used and only an irradiation period of 3 hours was considered. It should be checked to what extent these choices are critical. Because the ozone formation is not a linear function of time, the short irradiation time may underestimate the concentration for the cases with the lower radiation (see Figure 10). On the other hand an optimal hydrocarbon/NO_x ratio (on the ozone ridge, see Figure 11) will overestimate the concentrations relative to other mixing ratios.

The assumption of no additional emissions during the irradiation period also limits the interpretation of the results.

7. CONCLUSION AND RECOMMENDATIONS

This study has shown that the solar radiation potential for photochemical smog formation extends far north in the summer months. For example, the same or larger solar radiation potential exists at 60°N between the approximate dates April 25 and August 25 as in Los Angles on November 1st (Figures 12, 14, 16). Even at 70°N there is a considerable potential in the months May - July. In June the ozone level predicted at 60°N was 75 - 80% of that at 34°N. In the fall and spring the region of photochemical smog potential narrows. In September the predicted ozone level at 60°N was 35 - 40% of that at 34°N.

The northern latitudes can therefore not be excluded as future problem areas with regard to photochemical smog formation. This should be kept in mind when, for example, activities related to oil production are planned in Alaska and Norway, both of which are located approximately between 60°N and 70°N.

For all latitudes and months examined, the levels of peroxyacylnitrates and aldehydes were well correlated with the ozone level. The concentrations of peroxyacylnitrates were approximately one order of magnitude lower than those of ozone, while the aldehyde concentrations were of the same order of magnitude as those of ozone.

The time required to obtain the maximum NO_2 concentration was well correlated with the levels of ozone obtained, confirming that this time is an important variable in the photochemical smog cycle.

The magnitude of the NO_2 peak was not much influenced by variations in season and latitude and it decreased slightly when the solar flux increased.

This work may be continued by including other photolytic reactions in the reaction mechanism, for example the decomposition of ozone to singlet-D oxygen followed by reaction with water to hydroxyl radicals

$$O_3 + h\nu \rightarrow O(^1D) + O_2$$

$$O(^1D) + H_2O \rightarrow 2OH$$

The net effect is not necessarily a reduction in the ozone level because the hydroxyl radicals will react with hydrocarbons thus increasing the concentration of organic radicals being able to oxidize NO to NO_2. The photolysis of ozone can quite easily be included in the scheme and solved by the method outlined in this report by applying the steady state assumption to $O(^1D)$.

Another continuation of this work might be to check the results by using the new generalized mechanism of Whitten and Hogo (1976). This scheme does not include the ozone photolysis, but it includes the photolysis of formaldehyde to stable products:

$$HCHO + h\nu \rightarrow H_2 + CO$$

Also a solution method using Gear's algorithm should be used. Steady state assumptions can thus be avoided and the computing time can be substantially reduced.

The work should also be continued by using other initial mixtures and longer irradiation times.

REFERENCES

A. P. Altshuller and J. J. Bufalini, Photochemical Aspects of Air Pollution. A Review. Env. Sci. & Technol., Vol. 5, pp. 39-64 (1971).

A. Bemporad, Smithsonian Physical Tables. 9th Ed. Smithsonian Institution. Washington, D.C., p. 720 (1954).

F. E. Blacet and D. E. Loeffler, The Photolysis of Aliphatic Aldehydes. XI Acetaldehyde and Iodine Mixtures. J. Am. Chem. Soc., Vol. 64, pp. 893-896 (1942).

J. G. Calvert and J. N. Pitts, Photochemistry. John Wiley & Sons (1966).

J. G. Calvert, J. A. Kerr, K. L. Demerjian, and R. D. McQuigg, Photolysis of Formaldehyde as a Hydrogen Atom Source in the Lower Atmosphere. Science, Vol. 175, pp. 751-752 (1972).

J. G. Calvert, Test of the Theory of Ozone Generation in Los Angeles Atmosphere. Env. Sci. & Technol., Vol. 10, pp. 248-256 (1976).

K. J. Chu and J. H. Seinfeld, Formulation and Initial Application of a Dynamic Model for Urban Aerosols. Atm. Env., Vol. 9, pp. 375-402 (1975).

Climatic Impact Assessment Program. Monograph I, The Natural Stratosphere of 1974. U.S. Department of Transportation. Washington, D.C., 1975.

K. L. Demerjian, J. A. Kerr, J. G. Calvert, The Mechanism of Photochemical Smog Formation. Adv. in Env. Sci. & Technol., Vol. 4 pp. 1-262 (1974).

K. L. Demerjian and K. L. Schere, A Computer Program for Generating the Diurnal Variation of Photolytic Rate Constants for Atmospheric Pollutants. Presented at the International Conference on Environmental Sensing and Assessment, Las Vegas, Nevada, September 1975.

G. J. Doyle and N. A. Renzetti, J. Air Poll. Contr. Ass., Vol. 8, p. 23 (1958).

P. A. Durbin, T. A. Hecht, and G. Z. Whitten, Mathematical Modeling of Simulated Photochemical Smog. EPA-650/4-75-026, Environmental Protection Agency, Research Triangle Park, North Carolina (1975).

A. Q. Eschenroeder and J. R. Martinez, Concepts and Applications of Photochemical Smog Models. Advan. Chem., Vol. 113, pp. 101-168 (1972).

B.Finlayson, J.N. Pitts, Photochemistry of the Polluted Troposphere. Science, Vol. 192, pp. 111-119 (1976).

S. K. Friedlander and J. H. Seinfeld, A Dynamic Model of Photochemical Smog. Env. Sci. & Technol., Vol. 3, pp. 1175-1181 (1969).

C. W. Gear, The Automatic Integration of Ordinary Differential Equations. Communications of the ACM, Vol. 4, pp. 176-179 (1971).

W. A. Glasson and C. S. Tuesday, Hydrocarbon Reactivities in the Atmospheric Photooxidation of Nitric Oxide. Env. Sci. & Technol., Vol. 4, pp. 916-924 (1970).

R. Guicherit, Photochemical Smog Formation in The Netherlands. Proceedings of the Third International Clean Air Congress, Düsseldorf, West Germany, pp. C 98-101 (1973).

A. J. Haagen-Smit, Chemistry and Physiology of Los Angeles Smog. Ind. End. Chem., Vol. 44, pp. 1342-1346 (1952).

A. J. Haagen-Smit and M. M. Fox, Ind. Eng. Chem., Vol. 48, p. 1484 (1956).

R. W. Hamming, Numerical Methods for Scientists and Engineers. McGraw Hill. 411 p. (1962).

R. F. Hampson, Chemical Kinetics Data Survey. VI Photochemical and Rate Data for Twelve Gas Reactions of Interest for Atmospheric Chemistry. NBSIR 73-207, August 1973.

R. F. Hampson, Survey of Photochemical and Rate Data for Twenty-eight Reactions of Interest in Atmospheric Chemistry. J. Phys. Chem. Ref. Data, Vol. 2, pp. 267-312 (1973b)

R. F. Hampson and D. Garvin, Chemical Kinetic and Photochemical Data for Modelling Atmospheric Chemistry. NBS Technical Note 866, U.S. Department of Commerce, June 1975.

T. A. Hecht and J. H. Seinfeld, Development and Validation of a Generalized Mechanism for Photochemical Smog. Env. Sci. & Technol., Vol. 6, pp. 47-57 (1972).

T. A. Hecht, P. M. Roth and J. H. Seinfeld, Mathematical Simulation of Atmospheric Photochemical Reactions. Model Development, Validation and Application. EPA-650/4-74-011, Environmental Protection Agency, Research Triangle Park, North Carolina (1973).

T. A. Hecht, J. H. Seinfeld and M. C. Dodge, Further Development of Generalized Mechanism for Photochemical Smog. Env. Sci. & Technol., Vol. 8, pp. 327-339 (1974).

T. A. Hecht, M. K. Liu, and D. C. Whitney, Mathematical Simulation of Smog Chamber Photochemical Experiments. EPA-650/4-74-040, Environmental Protection Agency, Research Griangle Park, North Carolina (1974).

E. Hesstvedt, Formation of oxidants and other secondary pollutants in air mixed with nitrogen oxides and ethylene. Geophysica Norvegica, Vol. 31, No. 2, pp. 1-10 (1975).

E. Hesstvedt, Ø. Hov, and I. S. A. Isaksen, On the Chemistry of Mixtures of Hydrocarbons and Nitrogen Oxides in Air. Report No. 16, Institutt for Geofysikk, Universitetet i Oslo (1976).

E. C. Y. Inn and Y. Tanaka, J. Opt. Soc. Am., Vol. 43, p. 870 (1953).

F. S. Johnson, J. Meteorol., Vol. 11, p. 431 (1954).

H. S. Johnston and R. Graham, Photochemistry of NO_x and HNO_x Compounds. Can. J. Chem., Vol. 52, pp. 1415-1423 (1974).

P. A. Leighton, Photochemistry of Air Pollution. Academic Press (1961).

A. C. Lloyd, K. R. Darnall, A. M. Winer and J. N. Pitts, Relative Rate Constants for Reaction of the Hydroxyl Radical with a Series of Alkanes, Alkenes and Aromatic Hydrocarbons. J. Phys. Chem., Vol. 80, pp. 789-794 (1976).

P. Moon, J. Franklin Inst., Vol. 230, p. 583 (1940).

R. J. O'Brien, Photostationary State in Photochemical Smog Studies. Env. Sci. & Technol., Vol. 8, pp. 579-583 (1974).

J. T. Peterson and K. L. Demerjian, The Sensitivity of Computed Ozone Concentrations to U.V. Radiation in the Los Angeles Area. Atm. Env., Vol. 10, pp. 459-468 (1976).

J. N. Pitts, A. C. Lloyd, A. M. Winer, K. R. Darnall, and G. J. Doyle, Development and Application of a Hydrocarbon Reactivity Scale Based on Reaction with the Hydroxyl Radical. Presented at the 69th Annual Meeting of the Air Pollution Control Association, Portland, Oregon, June-July 1976.

S. D. Reynolds, P. M. Roth, and J. H. Seinfeld, Mathematical Modeling of Photochemical Air Pollution. I. Formulation of the Model. Atm. Env., Vol. 7, pp. 1033-1061 (1973).

E. A. Schuck, H. W. Ford, and E. R. Stephens, Air Pollution Effects of Irradiated Automobile Exhaust as Related to Fuel Consumption. Report No. 26, Air Pollution Foundation. San Marino, California (1958).

E. R. Stephens, E. F. Darley, O. C. Taylor, and W. E. Scott, Proc. Am. Petr. Inst., Vol. 40, No. III (1960).

H. C. Urey, L. H. Dawsey, and F. O. Rice, J. Am. Chem. Soc., Vol. 51, p. 1371 (1929).

K. Westberg and N. Cohen, The Chemical Kinetics of Photochemical Smog as Analyzed by Computer. AIR-70(8107)-1, The Aerospace Corp., El Segundo, California, December 1969.

G. Z. Whitten and H. H. Hogo, Mathematical Modeling of Simulated Photochemical Smog. EF76-126, Systems Applications Inc., San Rafael, California. Draft copy, August 1976.

Appendix A. The Hecht, Seinfeld and Dodge Photochemical Reaction Mechanism

No.	Reaction	Rate constant	Reference
1.	$NO_2 + h\nu \rightarrow NO + O$	Light dependent	This work
2.	$O + O_2 + M \rightarrow O_3 + M$	$2.1 \cdot 10^{-5}$ ppm^{-2} min^{-1}	Whitten and Hogo (1976)
3.	$O_3 + NO \rightarrow NO_2 + O_2$	25.2 ppm^{-1} min^{-1}	Whitten and Hogo (1976)
4.*	$O + NO + M \rightarrow NO_2 + M$		
5.	$O + NO_2 \rightarrow NO + O_2$	$1.34 \cdot 10^{4}$ ppm^{-1} min^{-1}	Whitten and Hogo (1976)
6.*	$O + NO_2 + M \rightarrow NO_3 + M$		
7.	$O_3 + NO_2 \rightarrow NO_3 + O_2$	$5.0 \cdot 10^{-2}$ ppm^{-1} min^{-1}	Whitten and Hogo (1976)
8.	$NO_3 + NO \rightarrow 2NO_2$	$1.3 \cdot 10^{4}$ ppm^{-1} min^{-1}	Whitten and Hogo (1976)
9.	$NO_3 + NO_2 \rightarrow N_2O_5$	$5.6 \cdot 10^{3}$ ppm^{-1} min^{-1}	Whitten and Hogo (1976)
10.	$N_2O_5 \rightarrow NO_2 + NO_3$	24.0 min^{-1}	Whitten and Hogo (1976)
11.	$N_2O_5 + H_2O \rightarrow 2HNO_3$	$5.0 \cdot 10^{-6}$ ppm^{-1} min^{-1}	Whitten and Hogo (1976)
12.*	$NO + HNO_3 \rightarrow HNO_2 + NO_2$		
13.*	$HNO_2 + HNO_3 \rightarrow H_2O + 2NO_2$		
14.	$NO + NO_2 + H_2O \rightarrow 2HNO_2$	$2.2 \cdot 10^{-9}$ ppm^{-2} min^{-1}	Whitten and Hogo (1976)
15.	$2HNO_2 \rightarrow NO + NO_2 + H_2O$	$1.3 \cdot 10^{-3}$ ppm^{-1} min^{-1}	Whitten and Hogo (1976)

Appendix A. (cont'd.)

No.	Reaction	Rate constant	Reference
16.	$HNO_2 + h\nu \rightarrow OH + NO$	Light dependent	This work
17.	$OH + NO_2 \rightarrow HNO_3$	$9.2 \cdot 10^3$ ppm^{-1} min^{-1}	Whitten and Hogo (1976)
18.	$OH + NO + M \rightarrow HNO_2 + M$	$9.0 \cdot 10^3$ ppm^{-1} min^{-1}	Whitten and Hogo (1976)
19.*	$OH + CO + (O_2) \rightarrow CO_2 + HO_2$		
20.	$HO_2 + NO \rightarrow OH + NO_2$	$2.0 \cdot 10^3$ ppm^{-1} min^{-1}	Whitten and Hogo (1976)
21.	$H_2O_2 + h\nu \rightarrow 2OH$	Light dependent	This work
22.	$HC_1 + O \rightarrow ROO + \alpha RCO_3 + (1-\alpha)HO_2$	$6.8 \cdot 10^3$ ppm^{-1} min^{-1}	Hecht, Seinfeld and Dodge (1974)
23.	$HC_1 + O_3 \rightarrow RCO_3 + RO + HC_4$	$1.6 \cdot 10^{-2}$ ppm^{-1} min^{-1}	Hecht, Seinfeld and Dodge (1974)
24.	$HC_1 + OH \rightarrow ROO + HC_4$	$4.2 \cdot 10^4$ ppm^{-1} min^{-1}	Lloyd et al. (1976)
25.*	$HC_2 + O \rightarrow ROO + OH$		
26.*	$HC_2 + OH \rightarrow ROO + H_2O$		
27.	$HC_3 + O \rightarrow ROO + OH$	65 ppm^{-1} min^{-1}	Hecht, Seinfeld and Dodge (1974)
28.	$HC_3 + OH \rightarrow ROO + H_2O$	$4.3 \cdot 10^3$ ppm^{-1} min^{-1}	Lloyd et al. (1976)
29.	$HC_4 + h\nu \rightarrow \beta ROO + (2-\beta)HO_2$	Light dependent	This work

Appendix A. (cont'd.)

No.	Reaction	Rate constant	Reference
30.	$HC_4 + OH \rightarrow \beta RCO_3 + (1-\beta)HO_2 + H_2O$	$2.3 \cdot 10^4$ ppm^{-1} min^{-1}	Hecht, Seinfeld and Dodge (1974)
31.	$ROO + NO \rightarrow RO + NO_2$	$9.1 \cdot 10^2$ ppm^{-1} min^{-1}	Hecht, Seinfeld and Dodge (1974)
32.	$RCO_3 + NO + (O_2) \rightarrow ROO+NO_2+CO_2$	$9.1 \cdot 10^2$ ppm^{-1} min^{-1}	Hecht, Seinfeld and Dodge (1974)
33.	$RCO_3 + NO_2 \rightarrow RCO_3NO_2$	$1.0 \cdot 10^2$ ppm^{-1} min^{-1}	Hecht, Seinfeld and Dodge (1974)
34.	$RO + O_2 \rightarrow HO_2 + HC_4$	$2.4 \cdot 10^{-2}$ ppm^{-1} min^{-1}	Hecht, Seinfeld and Dodge (1974)
35.	$RO + NO_2 \rightarrow RONO_2$	$4.9 \cdot 10^2$ ppm^{-1} min^{-1}	Hecht, Seinfeld and Dodge (1974)
36.	$RO + NO \rightarrow RONO$	$2.5 \cdot 10^2$ ppm^{-1} min^{-1}	Hecht, Seinfeld and Dodge (1974)
37.	$2HO_2 \rightarrow H_2O_2 + O_2$	$4.0 \cdot 10^3$ ppm^{-1} min^{-1}	Whitten and Hogo (1976)
38.*	$HO_2 + ROO \rightarrow RO + OH + O_2$		
39.*	$2ROO \rightarrow 2RO + O_2$		

*Reactions deleted in this work - see explanation in paragraphs 6.2.1 and 6.2.2.

Appendix A. (cont'd.)

HC_1 - alkenes (olefins)
HC_2 - aromatics
HC_3 - alkanes (paraffins)
HC_4 - aldehydes
RO - alkoxyl radicals
ROO - peroxyalkyl radicals
RCO_3 - peroxyacyl radicals
RONO - organic nitrites
$RONO_2$ - organic nitrates
$RCO_3\ NO_2$ - peroxyacylnitrates

α - Fraction of carbon attached to a monoalkene which are not terminal carbons.

β - Fraction of aldehydes which are not formaldehyde.

The notation O means $O(^3P)$.

Appendix B. Extinction coefficients (ℓ mole^{-1} cm^{-1}) and quantum yields for NO_2, HNO_2, H_2O_2, HCHO and CH_3CHO.

λ	NO_2		HNO_2		H_2O_2		HCHO		CH_3CHO	
nm	ε	ϕ	ε	ϕ	ε	ϕ	ε	ϕ	ε	ϕ
290	25.9	.988	0.0	1.0	3.9	1.0	8.33	.81	12.5	.35
300	36.9	.980	2.09	1.0	2.6	1.0	8.51	.66	11.0	.27
310	57.0	.972	3.24	1.0	1.8	1.0	8.23	.52	8.5	.20
320	78.0	.964	5.00	1.0	1.3	1.0	6.13	.40	5.2	.15
330	97.8	.956	7.40	1.0	0.8	1.0	6.19	.29	2.0	.07
340	118.8	.948	10.7	1.0	0.5	1.0	5.17	.18	0.5	0.0
350	136.0	.940	14.4	1.0	0.3	1.0	2.19	.09	0.0	0.0
360	148.9	.932	11.8	1.0	0.2	1.0	0.46	.01	0.0	0.0
370	158.0	.924	15.2	1.0	0.0	1.0	0.0	0.0	0.0	0.0
380	163.0	.916	8.87	1.0	0.0	1.0	0.0	0.0	0.0	0.0
390	166.9	.908	5.08	1.0	0.0	1.0	0.0	0.0	0.0	0.0
400	170.8	.76	0.71	1.0	0.0	1.0	0.0	0.0	0.0	0.0
410	166.9	.14	0.0	1.0	0.0	1.0	0.0	0.0	0.0	0.0
420	163.0	.07	0.0	1.0	0.0	1.0	0.0	0.0	0.0	0.0
430	153.8	.05	0.0	1.0	0.0	1.0	0.0	0.0	0.0	0.0
440	144.9	.04	0.0	1.0	0.0	1.0	0.0	0.0	0.0	0.0
Ref	Hampson (1973a)	Hampson and Garvin (1975)	Johnson and Graham (1974)	Demerjian and Schere (1975)	Urey et al. (1929)	Leighton (1961)	Calvert et al. (1972)	Calvert et al. (1972)	Calvert and Pitts (1966)	Blacet and Loeffler (1942)

Appendix C. Calculation of air mass (m) as a function of solar zenith angle (z).

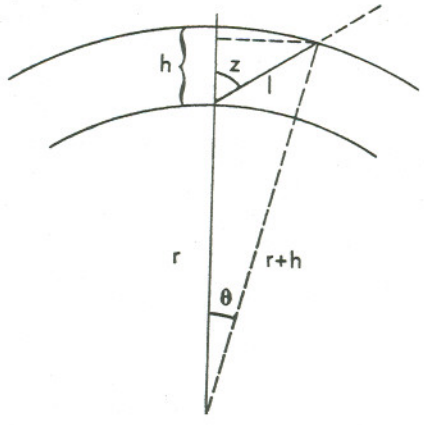

$m = \ell/h \geq 1$ air mass

Given:

r - radius of earth

h - thickness of atmosphere

z - solar zenith angle

Figure C1. Crossection of the earth and its atmosphere.

$$\ell^2 = r^2 + (r+h)^2 - 2r(r+h)\cos\Theta$$

$$r + \ell \cos z = (r+h)\cos\Theta$$

$$m = \ell/h$$

these equations determine m, ℓ and Θ

By introducing $\alpha = r/h$ and eliminating:

$$m^2 + 2\alpha\cos z \cdot m - (2\alpha+1) = 0$$

$$m = \sqrt{\alpha^2\cos^2 z + 2\alpha + 1} - \alpha\cos z$$

In this expression no attempt has been made to take the variation of density with height into account.

Appendix D. An algorithm for determining the background ozone content $[O_3]$ as a function of month (t) and latitude (lat) on the northern hemisphere.

From Figure 2 the values a, b, c and d in the expression

$$[O_3] = a \sin (bt-c) + d$$

were calculated for the latitudes 0°, 10°N, 20°N, ---, 90°N. These values were calculated from estimates of $[O_3]_{max}$, $[O_3]_{min}$ and the month at which the maximum and minimum occurred, t_{max} and t_{min} respectively.

$$[O_3]_{max} - [O_3]_{min} = 2a$$

$$[O_3]_{max} = a+d$$

$$bt_{max}-c = 90$$

$$bt_{min}-c = 270$$

The values are summarized in Table D1.

The coefficients a, b, c and d were then plotted as a function of latitude and suitable mathematical expressions were chosen to fit the data. The coefficient b was held constant. The plots for a, c and d are shown in Figures D1-3 together with the fitting curves. A "hockey-stick" linear regression analysis was done for coefficient a giving

$$a = 0.10 \text{ for lat} < 11.4°$$

$$a = 0.0092 \cdot \text{lat} - 0.005 \text{ for lat} > 11.4°$$

A piece-wise linear regression analysis was done for coefficient c giving

Table D1. Estimation of the coefficients a, b, c and d in the expression $[O_3] = a \sin (bt-c) + d$

Latitude °N	$[O_3]_{max}$ (mm STP)	$[O_3]_{min}$ (mm STP)	t_{max} (mo.)	t_{min} (mo.)	a	b	c	d
90	4.50	2.90	3.8	9.8	0.80	30	24	3.70
80	4.45	2.95	3.8	9.8	0.75	30	24	3.70
70	4.30	3.05	3.8	9.8	0.62	30	24	3.68
60	4.20	3.05	3.8	9.8	0.58	30	24	3.62
50	3.90	2.95	3.8	9.8	0.48	30	24	3.42
40	3.60	2.85	4.0	10.0	0.38	30	30	3.22
30	3.20	2.70	4.2	10.2	0.25	30	36	2.95
20	2.90	2.60	4.4	10.4	0.15	30	42	2.75
10	2.75	2.55	5.0	11.0	0.10	30	60	2.65
0	2.70	2.50	6.0	12.0	0.10	30	90	2.60

$c = -3\ lat + 90$ for $lat < 15°$

$c = -0.6\ lat + 54$ for $15° < lat < 50°$

$c = 24$ for $lat > 50°$

A sine-function was fitted to the coefficient d for latitudes below 75° while d was kept constant for latitudes above 75°:

$d = 0.55 \sin(2.40\ lat - 90) + 3.15$ for $lat < 75°$

$d = 3.70$ for $lat > 75°$

This algorithm gives ozone values shown in figure D4. The isopleths correspond quite well with Figure 2. The choice of background ozone concentration, however, is not critical for the resulting rate constants. If a constant $[O_3]$ = 2.2 mm STP was used for all months and all latitudes, the maximum increase in the rate constants would be about 1%.

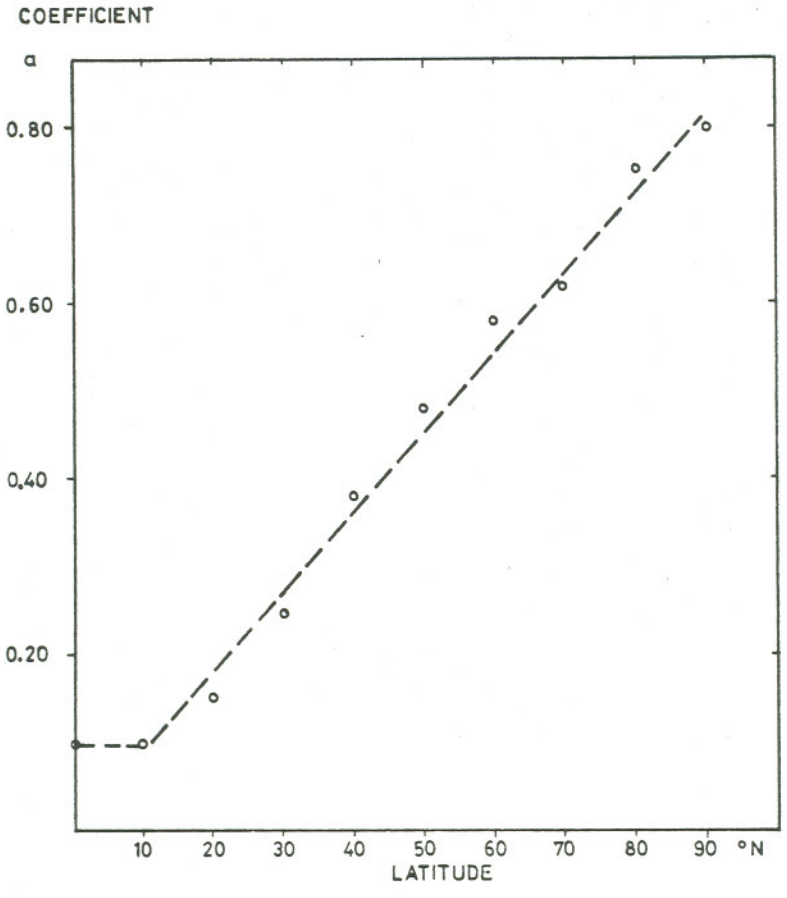

Figure D1. Coefficient a as a function of latitude.

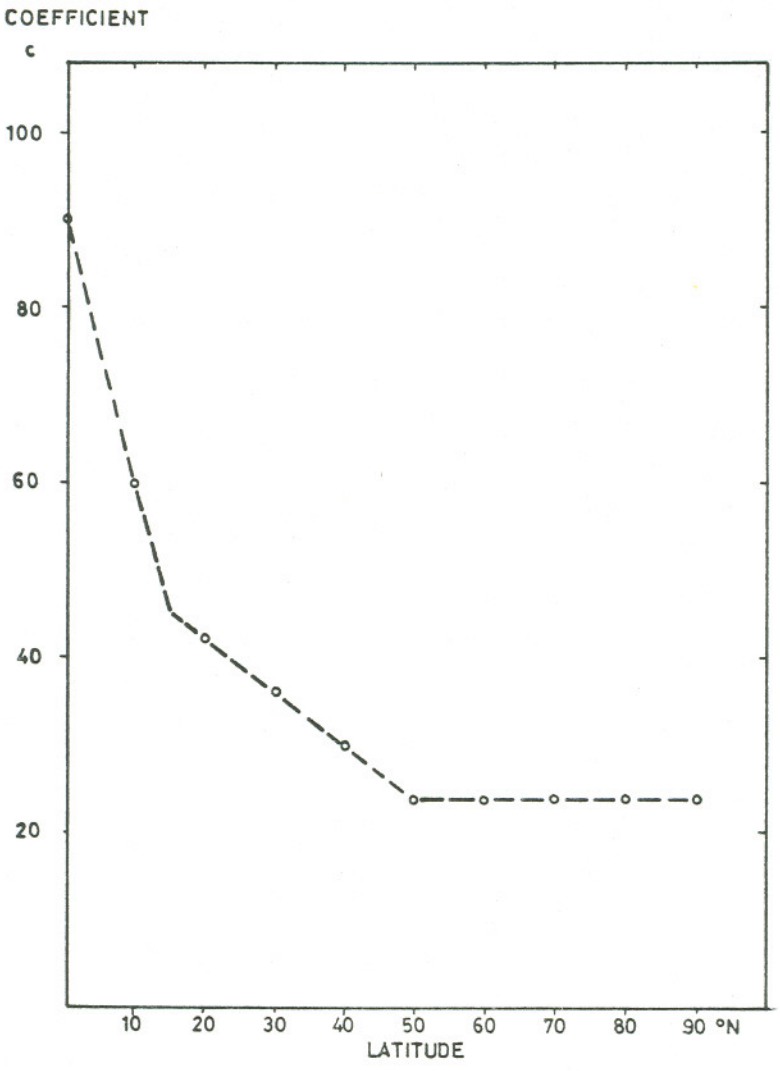

Figure D2. Coefficient c as a function of latitude.

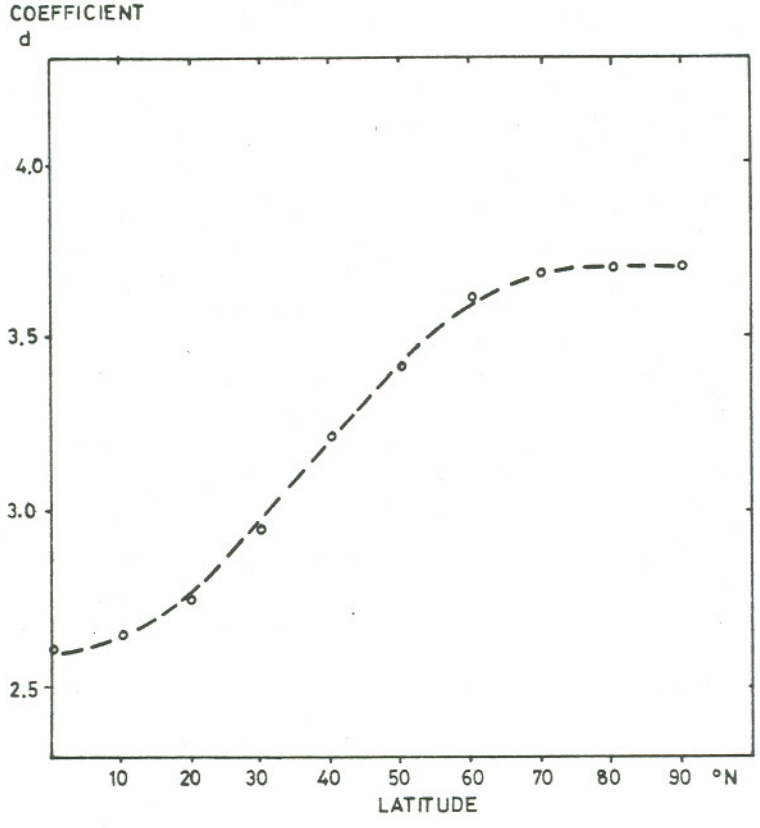

Figure D3. Coefficient d as a function of latitude.

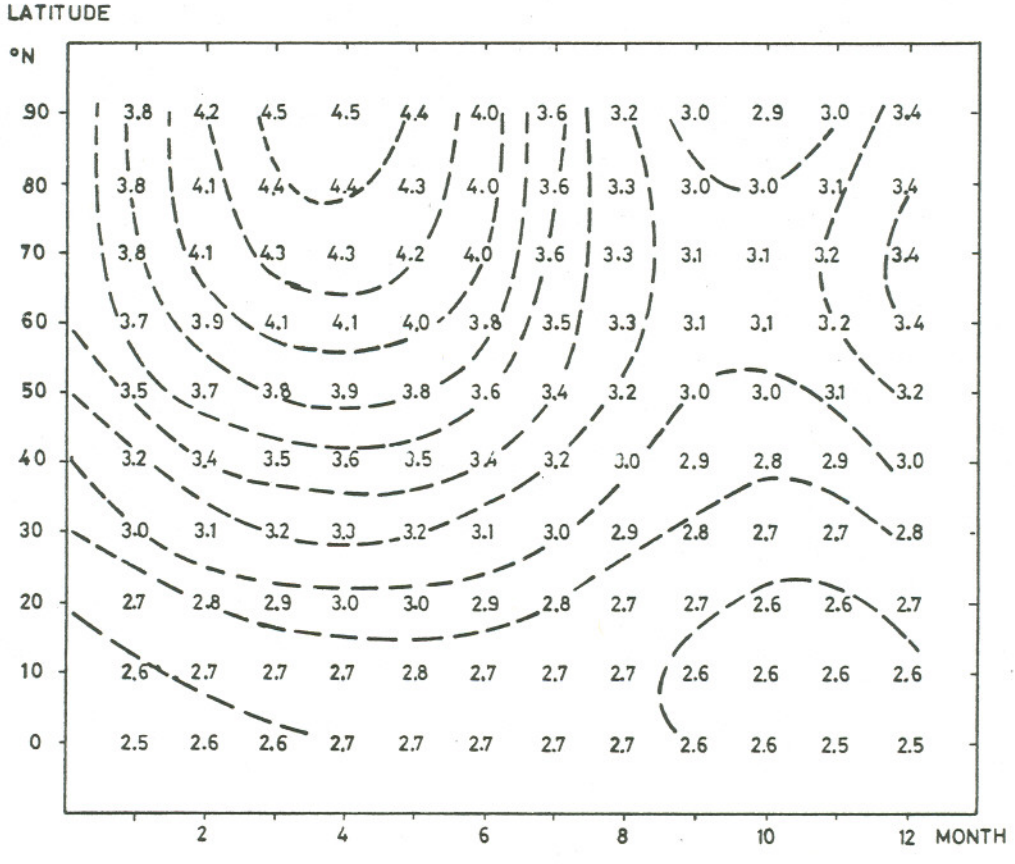

Figure D4. Computed values of the background ozone content (mm STP) as a function of month and latitude.

Appendix E. The computer program used in this work.

```
C  FURTHER MODIFIED 30 STEP HECHT ET AL. PHOTOCHEMICAL MECHANISM.

C  FURTHER MODIFIED 30 STEP HECHT ET AL. PHOTOCHEMICAL MECHANISM.
C  REACTIONS NO. 4, 6, 12, 13, 19, 25, 26, 38 AND 39 IS ELIMINATED FROM
C  THE ORIGINAL HECHT, SEINFELD AND DODGE MODEL, PUBLISHED IN
C  ENV. SCI. & TECHNOL., VOL. 8, NO. 4, PP. 327-339, (1974).
C
C  THE FOLLOWING RATE CONSTANTS HAVE BEEN UPDATED:
C  1,2,3,5,7,8,9,10,11,14,15,16,17,18,   20,21,24,28,29,37.
C
C  A MODIFIED HAMMING'S PREDICTOR-CORRECTOR CODE WITH VARIABEL
C  STEP LENGTH IS USED FOR THE INTEGRATION.
C  THE FOLLOWING COMPONENTS ARE STEADY-STATED:
C  O, NO3, HO2, OH, RO, ROO, RCOOO.
C
      DIMENSION Y(11),DERY(11),AUX(16,11),PRMT(5)
      DOUBLE PRECISION Y,DERY,AUX,PRMT
      DOUBLE PRECISION ALFA,BETA,C1,C2,C3,C4,C5,C6,C7,C8,C9,C10,C11,C12,
     &   C13,C14,C15,C16,C17,C18,C19,C20,C21,C22,C23,C24,C25,C26,C27,
     &   C28,C29,C30,C31,C32,C33,C34,C35,C36,C37,C38,C39
      COMMON ALFA,BETA,C1,C2,C3,C4,C5,C6,C7,C8,C9,C10,C11,C12,C13,C14,
     &   C15,C16,C17,C18,C19,C20,C21,C22,C23,C24,C25,C26,C27,C28,
     &   C29,C30,C31,C32,C33,C34,C35,C36,C37,C38,C39
      DOUBLE PRECISION O, NO3, HO2, OH, RO, ROO, RCOOO
      COMMON /ST/ IOUT, O, NO3, HO2, OH, RO, ROO, RCOOO
      COMMON /OUT/ STEP, DSTEP, TINT
      DOUBLE PRECISION O2,M,H2O
      COMMON /COM/ ISW,IFLAG, N
      COMMON /LYS/ AZEN,BZEN,TSTART,RAD,FACT,OZONEC
      EXTERNAL FCT, OUTP
C
C  VALIDATION VALUES FOR RATE CONSTANTS AND STOCHIOMETRIC COEFFICIENTS.
C  STOCHIOMETRIC COEFFICIENTS ARE FOR PROPYLENE/N-BUTHANE.
C
      DATA C1,C2,C3,C4,C5/0.2660D0,2.1D-5,25.2D0,3.5D-3,1.34D+4/,
     &   C6,C7,C8,C9,C10/2.2D-3,5.0D-2,1.3D+4,5.6D+3,2.4D+1/,
     &   C11,C12,C13,C14,C15/5.0D-6,2.5D-4,0.2D0,2.2D-3,1.3D-3/,
     &   C16,C17,C18,C19,C20/1.3D-2,9.2D+3,9.0D+3,2.1D+2,2.0D+3/,
     &   C21,C22,C23,C24,C25/1.064D-3,6.8D+3,1.6D-2,4.2D+4,1.07D+2/,
     &   C26,C27,C28,C29,C30/8.0D+3,6.5D+1,4.3D+3,2.5D-3,2.3D+4/,
     &   C31,C32,C33,C34,C35/9.1D+2,9.1D+2,1.0D+2,2.4D-2,4.9D+2/,
     &   C36,C37,C38,C39/2.5D+2,4.0D+3,1.0D+2,1.0D+2/
      DATA ALFA,BETA/0.5D0,0.63D0/
C
      DATA O2,M,H2O/20.9D+4,1.0D+6,15.0D+3/
      DATA PI/3.141592653/, AVOGAD/6.024E+23/
C
      FACT = 2.303 * 1000.0 * 60.0 / AVOGAD
      RAD = PI / 180.0
      TINT = -1.0
      STEP = 0.0
C
C  CONTROL PARAMETERS AND INITIALIZATION.
C
      NDIM = 11
      DSTEP =  5.0
      PRMT(1) = 0.0D0
      PRMT(2) = 180.0D0
```

```
C  FURTHER MODIFIED 30 STEP HECHT ET AL. PHOTOCHEMICAL MECHANISM.

      PRMT(3) = 0.1D0
      PRMT(4) = 0.001D0
C
      AMONTH = 6.0
      XLAT = 60.0
      TSTART = 9.00
C
      XDIM = NDIM
      DO 4 I = 1,NDIM
      DERY(I) = 1.0D0/XDIM
    4 Y(I) = 0.0D0
C
C  MULTIPLICATION OF RATE CONSTANTS BY CONSTANT CONCENTRATIONS.
C
      C2 = C2 * O2 * M
      C4 = C4 * M
      C6 = C6 * M
      C11 = C11 * H2O
      C14 = C14 * H2O
      C34 = C34 * O2
C
C  CALCULATION OF DECLINATION (DEC) AND ATMOSPHERIC OZONE CONTENT
C  (OZONEC) AS A FUNCTION OF MONTH (AMONTH).
C
      DEC = 23.5 * SIN((30.0*AMONTH-90.0)*RAD)
      DEC = DEC*RAD
      CALL TOZONE(XLAT,AMONTH,OZONEC,RAD)
      XLAT = XLAT * RAD
      AZEN = COS(XLAT) * COS(DEC)
      BZEN = SIN(XLAT) * SIN(DEC)
C
C  ASSIGNMENT OF INITIAL CONCENTRATIONS.
C
      Y(2) = 0.15D0
      Y(3) = 0.1D0
      Y(8) = 0.15D0
      Y(9) = 0.45D0
C
      CALL SEARCH(2,'OUTPUT',2,0)
      CALL DHPCG(PRMT,Y,DERY,NDIM,IHLF,FCT,OUTP,AUX)
      WRITE(6,2000) IHLF
 2000 FORMAT(1H ,5X,5HIHLF=,I2)
      CALL SEARCH(4,0,2,0)
      CALL EXIT
      END
C
      SUBROUTINE FCT(X,Y,DERY)
      DIMENSION Y(1),DERY(1)
      DOUBLE PRECISION X,Y,DERY
      COMMON ALFA,BETA,C1,C2,C3,C4,C5,C6,C7,C8,C9,C10,C11,C12,C13,C14,
     &   C15,C16,C17,C18,C19,C20,C21,C22,C23,C24,C25,C26,C27,C28,
     &   C29,C30,C31,C32,C33,C34,C35,C36,C37,C38,C39
      DOUBLE PRECISION ALFA,BETA,C1,C2,C3,C4,C5,C6,C7,C8,C9,C10,C11,C12,
     &   C13,C14,C15,C16,C17,C18,C19,C20,C21,C22,C23,C24,C25,C26,C27,
     &   C28,C29,C30,C31,C32,C33,C34,C35,C36,C37,C38,C39
      COMMON /ST/ IOUT, O, NO3, HO2, OH, RO, RO0, RC000
```

```
C  FURTHER MODIFIED 30 STEP HECHT ET AL. PHOTOCHEMICAL MECHANISM.

      INTEGER I, IOUT
      REAL TMIN,ZSTEP
      DOUBLE PRECISION O, NO3, NO2, OH, RO, ROO, RCOOO
      DOUBLE PRECISION
      DATA ZSTEP/0.0/
C
C  CALCULATION OF TIME DEPENDENT PHOTOLYTIC RATE CONSTANTS.
C
      TMIN = X
      IF (TMIN .LT. ZSTEP) GO TO 10
      ZSTEP = ZSTEP + 1.0
      CALL PHOTO(TMIN)
   10 CONTINUE
C
C  GENERATION OF SINGLE, NON-NEGATIVE VARIABLES.
C
      O3 = DMAX1(Y(1),0.0D0)
      NO = DMAX1(Y(2),0.0D0)
      NO2 = DMAX1(Y(3),0.0D0)
      N2O5 = DMAX1(Y(4),0.0D0)
      HNO2 = DMAX1(Y(5),0.0D0)
      HNO3 = DMAX1(Y(6),0.0D0)
      H2O2 = DMAX1(Y(7),0.0D0)
      HC1 = DMAX1( Y(8),0.0D0)
      HC3 = DMAX1(Y(9), 0.0D0)
      HC4 = DMAX1(Y(10),0.0D0)
      PAN = DMAX1(Y(11),0.0D0)
C
C  CALCULATION OF COMPLETE REACTION RATES.
C
      R1 = C1 * NO2
      R3 = C3 * O3 * NO
      R7 = C7 * O3 * NO2
      R10 = C10 * N2O5
      R11 = C11 * N2O5
      R14 = C14 * NO * NO2
      R15 = C15 * HNO2 * HNO2
      R16 = C16 * HNO2
      R21 = C21 * H2O2
      R23 = C23 * HC1 * O3
      R29 = C29 * HC4
C
C  CALCULATION OF INCOMPLETE REACTION RATES FOR
C  STEADY STATE APPROXIMATIONS.
C
      R5 = C5 * NO2
      R8 = C8 * NO
      R9 = C9 * NO2
      R17 = C17 * NO2
      R18 = C18 * NO
      R20 = C20 * NO
      R22 = C22 * HC1
      R24 = C24 * HC1
      R27 = C27 * HC3
      R28 = C28 * HC3
      R30 = C30 * HC4
```

```
C  FURTHER MODIFIED 30 STEP HECHT ET AL. PHOTOCHEMICAL MECHANISM.

      R31 = C31 * NO
      R32 = C32 * NO
      R33 = C33 * HO2
      R35 = C35 * HO2
      R36 = C36 * NO
C
C  STEADY STATE APPROXIMATIONS AND
C  COMPLETION OF INCOMPLETE REACTION RATES.
C
      O = R1 / (C2+R5+R22+     R27)
C
      R2 = C2 * O
      R5 = R5 * O
      R22 = R22 * O
      R27 = R27 * O
C
      HO3 = (R7+R10) / (R8+R9)
C
      R8 = R8 * HO3
      R9 = R9 * HO3
C
C     STEADY STATE OF HO2.
      B = R32 / (R32+R33)
      A = R22 + R23 +        R27 + BETA*R29 + B*(ALFA*R22+R23)
      B = R24 +        R28 + BETA*R30*B
      C = C34 + R35 + R36
      D = R16 + 2.0D0*R21 +        R27
      E = R17 + R18 +        R24 +        R28 + R30
      F = (1.0D0-ALFA)*R22 + (2.0D0-BETA)*R29
      G =        (1.0D0-BETA)*R30
      H = (G + C34*B/C) / E
      U = R20*(1.0D0-H)
      V = F + C34*A/C + D*H
      HO2 = (DSQRT(U*U+4.0D0*C37*V) - U) / (2.0D0*C37)
C
      R20 = R20 * HO2
      R37 = C37 * HO2 * HO2
C
      OH = (D + R20) / E
C
C
      R17 = R17 * OH
      R18 = R18 * OH
      R24 = R24 * OH
      R28 = R28 * OH
      R30 = R30 * OH
C
      RC000 = (R22*ALFA+R23+R30*BETA) / (R32+R33)
C
      R32 = R32 * RC000
      R33 = R33 * RC000
C
      R00 = (R22+R24+        R27+R28+R29*BETA+R32) / R31
C
      R31 = R31 * R00
C
```

```
C  FURTHER MODIFIED 30 STEP HECHT ET AL. PHOTOCHEMICAL MECHANISM.


      RO = (R23+R31) / C
C
      R34 = C34 * RO
      R35 = R35 * RO
      R36 = R36 * RO
C
C  RETURN IF FCT IS CALLED FROM OUTP.
C
      IF (IOUT .EQ. 1) RETURN
C
C  CALCULATION OF DERIVATIVES.
C
      DERY(1) = R2 - R3 - R7 - R23
      DERY(2) = R1+R5+R15+R16 - R3    -R8     -R14-R18-R20-R31-R32-R36
      DERY(3) = R3   +2.D0*R8+R10            +R15+R20+R31+R32
     &         -R1-R5    -R7-R9-R14-R17-R33-R35
      DERY(4) = R9 - R10 - R11
      DERY(5) =     + 2.D0*R14 + R18        - 2.D0*R15 - R16
      DERY(6) = 2.D0*R11 + R17
      DERY(7) = R37 - R21
      DERY(8)  = - R22 - R23 - R24
      DERY(9)  = - R27 - R28
      DERY(10) = R23 + R24 + R34 - R29 - R30
      DERY(11) = R33
C
C  GENERATION OF NON-NEGATIVE DERIVATIVES FOR NON-POSITIVE Y-VALUES.
C
      DO 50 I = 1,11
   50 IF (Y(I) .LE. 0.0D0) DERY(I) = DMAX1(DERY(I),0.0D0)
C
C  GENERATION OF NON-NEGATIVE Y-VALUES.
C
      DO 60 I = 1,11
   60 Y(I) = DMAX1(Y(I),0.0D0)
C
      RETURN
      END
C
      SUBROUTINE OUTP(X,Y,DERY,IHLF,NDIM,PRMT)
      DIMENSION Y(1),DERY(1),PRMT(1)
      DOUBLE PRECISION X,Y,DERY,PRMT
      COMMON ALFA,BETA,C1,C2,C3,C4,C5,C6,C7,C8,C9,C10,C11,C12,C13,C14,
     &   C15,C16,C17,C18,C19,C20,C21,C22,C23,C24,C25,C26,C27,C28,
     &   C29,C30,C31,C32,C33,C34,C35,C36,C37,C38,C39
      DOUBLE PRECISION ALFA,BETA,C1,C2,C3,C4,C5,C6,C7,C8,C9,C10,C11,C12,
     &   C13,C14,C15,C16,C17,C18,C19,C20,C21,C22,C23,C24,C25,C26,C27,
     &   C28,C29,C30,C31,C32,C33,C34,C35,C36,C37,C38,C39
      COMMON /ST/ IOUT, O, NO3, HO2, OH, RO, ROO, RCOOO
      DOUBLE PRECISION O, NO3, HO2, OH, RO, ROO, RCOOO
      COMMON /COM/ ISW,IFLAG, N
      COMMON /OUT/ STEP, DSTEP, TINT
      TINT = TINT + 1.0
      XX = X
      IF (XX .LT. STEP) RETURN
      STEP = STEP + DSTEP
      WRITE(6,1999)
```

```
C  FURTHER MODIFIED 30 STEP HECHT ET AL. PHOTOCHEMICAL MECHANISM.

      WRITE(6,2000) X, IHLF, TINT
      WRITE(6,1999)
      WRITE(6,2001) (Y(I),I=1,6)
      WRITE(6,2001) (Y(I),I=7,11)
      IOUT = 1
      CALL FCT(X,Y,DERY)
      IOUT = 0
      WRITE(6,1999)
      WRITE(6,2002) O, NO3, HO2, OH, RO, ROO, RCOOO
      WRITE(6,1999)
      WRITE(6,2003) C1,   C16,C21,C29
 1999 FORMAT(1H.)
 2000 FORMAT(1H ,1X,22HX-VALUE AND PARAMETERS,F9.3,I9,F10.0)
 2001 FORMAT(1H ,3X,8HY-VALUES, 6D13.4)
 2002 FORMAT(1H ,3X, 12HSTEADY STATE,9X,7D13.4)
 2003 FORMAT(1H ,3X,14HRATE CONSTANTS,7X,4D13.4)
      RETURN
      END
C
      SUBROUTINE PHOTO(TMIN)
C
C  CALCULATION OF PHOTOLYTIC RATE CONSTANTS FOR ATMOSPHERIC POLLUTANTS.
C
      COMMON /LYS/ AZEN,BZEN,TSTART,RAD,FACT,OZONEC
      COMMON ALFA,BETA,C1,C2,C3,C4,C5,C6,C7,C8,C9,C10,C11,C12,C13,C14,
     &   C15,C16,C17,C18,C19,C20,C21,C22,C23,C24,C25,C26,C27,C28,
     &   C29,C30,C31,C32,C33,C34,C35,C36,C37,C38,C39
      DOUBLE PRECISION ALFA,BETA,C1,C2,C3,C4,C5,C6,C7,C8,C9,C10,C11,C12,
     &   C13,C14,C15,C16,C17,C18,C19,C20,C21,C22,C23,C24,C25,C26,C27,
     &   C28,C29,C30,C31,C32,C33,C34,C35,C36,C37,C38,C39
C
      DIMENSION RADO(16),SMO(16),RADJ(16), TA(16),TMLG(16),TPLG(16),
     .          TS(16), ALOZ(16)
      DIMENSION EXNO2(16),FINO2(16),EXHNO2(16),FIHNO2(16),EXH2O2(16),
     .          FIH2O2(16),EXFAL(16),FIFAL(16),EXACAL(16),FIACAL(16)
      DATA RADO/7.6, 9.2, 11.9, 13.7, 19.1, 19.0, 20.7, 21.0, 24.8,
     .          23.6, 22.0, 31.0, 40.1, 40.6, 38.6, 45.0/
      DATA SMO/0.613, 0.530, 0.461, 0.402, 0.353, 0.311, 0.275, 0.245,
     .         0.218, 0.195, 0.175, 0.158, 0.142, 0.129, 0.117, 0.106/
      DATA ALOZ/1.66, 0.44, 0.12, 0.032, 0.0085, 0.0020, 0.0005, 9*0.0/
      DATA IMAX/16/, GG,XXI,WW,DD/0.5, 2.0, 2.0, 1.0/
      DATA PRAT/1.0/
      DATA RELAT/600.0/
      DATA EXNO2 /25.9,36.9,57.0,78.0,97.8,118.8,136.0,148.9,158.0,
     .           163.0,166.9,170.8,166.9,163.0,153.8,144.9/
      DATA FINO2 /.988,.980,.972,.964,.956,.948,.940,.932,.924,.916,
     .           .908,.76,.14,.07,.05,.04/
      DATA EXHNO2 /0.00,2.09,3.24,5.0,7.4,10.7,14.4,11.8,15.2,8.87,
     .            5.08,0.71,4*0.0/
      DATA FIHNO2 /16*1.0/
      DATA EXH2O2 /3.9,2.6,1.8,1.3,1.0,0.8,0.5,0.3,0.2,7*0.0/
      DATA FIH2O2 /16*1.0/
      DATA EXFAL/8.33,8.51,8.23,6.13,6.19,5.17,2.19,0.46,8*0.0/
      DATA FIFAL/0.81,0.66,0.52,0.40,0.29,0.18,0.09,0.01,8*0.0/
      DATA EXACAL/12.5,11.0,8.5,5.2,2.0,0.5,10*0.0/
      DATA FIACAL/0.35,0.27,0.20,0.15,0.07,11*0.0/
```

```
C  FURTHER MODIFIED 30 STEP HECHT ET AL. PHOTOCHEMICAL MECHANISM.

C
      TIME = TSTART + TMIN/60.0
      XLHA = (TIME-12.0) * 15. * RAD
C
C  CALCULATION OF SOLAR ZENITH ANGLE (ZENANG) AS A FUNCTION OF
C  DECLINATION (DEC), LATITUDE (XLAT) AND LOCAL HOUR ANGLE (XLHA).
C  ZCOS IS EQUAL TO COS(ZENANG).
C
      ZCOS = AZEN*COS(XLHA) + BZEN
C
C  INITIALIZATION OF RATE CONSTANTS.
C
      RNO2  = 0.0
      RHNO2 = 0.0
      RH2O2 = 0.0
      RFAL  = 0.0
      RACAL = 0.0
      IF (ZCOS .LE. 0.0) GO TO 150
C
C  CALCULATION OF AIR MASS AS A FUNCTION OF SOLAR ZENITH ANGLE
C
      ZSEN = RELAT * ZCOS
      AIRMAS = SQRT(ZSEN*ZSEN + 2.*RELAT + 1.) - ZSEN
C
      DO 100 I = 1,IMAX
      XLAMB = 2800 + 100*I
C
C  CALCULATION OF TRANSMISSION FROM ABSORPTION OF OZONE
C
      TA(I) = 10.**(-ALOZ(I)*OZONEC*AIRMAS)
C
C  CALCULATION OF TRANSMISSION (LOGARITHMIC) FROM MOLECULAR SCATTERING
C
      TMLG(I) = -SMO(I) * PRAT * AIRMAS
C
C  CALCULATION OF TRANSMISSION (LOGARITHMIC) FROM PARTICULATE DIFFUSION
C
      XLAMB = XLAMB / 10000.0
      TPLG(I) = -(0.375*XLAMB**(-2.)*UW + 3.5*XLAMB**(-0.75)*DD)*
     .          AIRMAS / 100.0
      XLAMB = XLAMB * 10000.0
C
C  CALCULATION OF TRANSMISSION FROM MOLECULAR SCATTERING AND
C  PARTICULATE DIFFUSION
C
      TS(I) = 10.**(TMLG(I)+TPLG(I))
C
C  ESTIMATED ACTINIC IRRADIANCE IN THE LOWER ATMOSPHERE
C
      RADJ(I) = RADO(I)*TA(I)*(TS(I) + GG*XXI*(1.-TS(I))*ZCOS) *1.0E+14
C
  100 CONTINUE
C
C  CALCULATION OF RATE CONSTANTS AS A FUNCTION OF SOLAR RADIATION,
C  EXTINCTION COEFFICIENTS AND QUANTUM YIELDS
C
```

```
C  FURTHER MODIFIED 30 STEP HECHT ET AL. PHOTOCHEMICAL MECHANISM.

      DO 120 I = 1,IMAX
      RNO2  = RNO2  + RADJ(I)*EXNO2 (I)*FINO2 (I)
      RHNO2 = RHNO2 + RADJ(I)*EXHNO2(I)*FIHNO2(I)
      RH2O2 = RH2O2 + RADJ(I)*EXH2O2(I)*FIH2O2(I)
      RFAL  = RFAL  + RADJ(I)*EXFAL (I)*FIFAL (I)
      RACAL = RACAL + RADJ(I)*EXACAL(I)*FIACAL(I)
  120 CONTINUE
      RNO2  = RNO2  * FACT
      RHNO2 = RHNO2 * FACT
      RH2O2 = RH2O2 * FACT
      RFAL  = RFAL  * FACT
      RACAL = RACAL * FACT
C
  150 CONTINUE
C
      C1 = RNO2
      C16 = RHNO2
      C21 = RH2O2
      C29 = RFAL*(1.0D0-BETA) + RACAL*BETA
C
      RETURN
      END
C
      SUBROUTINE TOZONE(XLAT,AMONTH,OZONEC,RAD)
C
C  THIS SUBROUTINE GIVES THE BACKGROUND ATMOSPHERIC OZONE CONTENT
C  (OZONEC) IN MM STP AS A FUNCTION OF LATITUDE (XLAT) AND MONTH
C  (AMONTH)
C
      B = 30.0
      IF (XLAT - 11.4) 5, 5, 6
    5 A = 0.10
      C = -3.0*XLAT + 90.0
      D = 0.55*SIN((2.40*XLAT-90.0)*RAD) + 3.15
      GO TO 20
    6 A = 0.0092*XLAT - 0.005
      IF (XLAT - 15.0) 7, 7, 8
    7 C = -3.0*XLAT + 90.0
      D = 0.55*SIN((2.40*XLAT-90.0)*RAD) + 3.15
      GO TO 20
    8 IF (XLAT - 50.0) 9, 9, 10
    9 C = -0.6*XLAT + 54.0
      D = 0.55*SIN((2.40*XLAT-90.0)*RAD) + 3.15
      GO TO 20
   10 C = 24.0
      IF (XLAT - 75.0) 11, 11, 12
   11 D = 0.55*SIN((2.40*XLAT-90.0)*RAD) + 3.15
      GO TO 20
   12 D = 3.70
   20 CONTINUE
      OZONEC = A * SIN((B*AMONTH-C)*RAD) + D
      RETURN
      END
```

MONTH	1	2	3	4	5	6	7	8	9	10	11	12
LATITUDE												
90.	0.00	0.00	0.00	1.32	2.51	2.92	2.52	1.33	0.00	0.00	0.00	0.00
80.	0.00	0.00	1.08	2.69	3.68	4.00	3.70	2.71	1.10	0.00	0.00	0.00
70.	0.00	0.86	2.46	3.82	4.56	4.79	4.58	3.85	2.48	0.87	0.00	0.00
60.	1.04	2.23	3.65	4.67	5.20	5.36	5.21	4.69	3.68	2.25	1.05	0.66
50.	2.43	3.48	4.55	5.27	5.64	5.76	5.66	5.30	4.58	3.50	2.44	2.00
40.	3.64	4.43	5.20	5.70	5.94	6.01	5.96	5.72	5.22	4.45	3.65	3.30
30.	4.55	5.12	5.66	5.98	6.12	6.15	6.13	6.00	5.67	5.13	4.56	4.30
20.	5.21	5.61	5.96	6.14	6.18	6.18	6.19	6.15	5.97	5.62	5.22	5.03
10.	5.67	5.93	6.14	6.19	6.13	6.09	6.13	6.19	6.14	5.94	5.67	5.55
0.	5.97	6.13	6.20	6.12	5.96	5.88	5.96	6.12	6.20	6.13	5.97	5.89

Appendix F. Rate constant for $NO_2 + h\nu \rightarrow NO + O(^3P)$ as a function of month and latitude
Units: 10^{-1} min^{-1} Local time: 1200

MONTH	1	2	3	4	5	6	7	8	9	10	11	12
LATITUDE												
90.	0.00	0.00	0.00	1.32	2.51	2.92	2.52	1.33	0.00	0.00	0.00	0.00
80.	0.00	0.00	0.72	2.28	3.35	3.69	3.37	2.31	0.73	0.00	0.00	0.00
70.	0.00	0.25	1.63	3.13	4.00	4.27	4.02	3.16	1.65	0.25	0.00	0.00
60.	0.16	1.06	2.56	3.80	4.48	4.70	4.50	3.83	2.58	1.07	0.17	0.00
50.	0.99	2.03	3.34	4.30	4.82	4.98	4.83	4.33	3.36	2.05	0.99	0.65
40.	2.00	2.94	3.95	4.66	5.03	5.14	5.04	4.68	3.97	2.95	2.01	1.64
30.	2.95	3.66	4.39	4.88	5.12	5.19	5.13	4.90	4.41	3.68	2.96	2.66
20.	3.72	4.22	4.70	4.99	5.10	5.12	5.11	5.00	4.71	4.22	3.72	3.50
10.	4.30	4.61	4.88	4.99	4.97	4.94	4.97	4.99	4.88	4.61	4.30	4.15
0.	4.71	4.87	4.94	4.86	4.70	4.62	4.70	4.86	4.94	4.87	4.71	4.63

Appendix F. (cont'd.) Rate constant for $NO_2 + h\nu \rightarrow NO + O(^3P)$ as a function of month and latitude
Units: 10^{-1} min^{-1} Local time: 0900

MONTH	1	2	3	4	5	6	7	8	9	10	11	12
LATITUDE												
90.	0.00	0.00	0.00	1.32	2.51	2.92	2.52	1.33	0.00	0.00	0.00	0.00
80.	0.00	0.00	0.00	1.29	2.46	2.87	2.48	1.31	0.00	0.00	0.00	0.00
70.	0.00	0.00	0.00	1.22	2.34	2.73	2.35	1.23	0.00	0.00	0.00	0.00
60.	0.00	0.00	0.00	1.11	2.13	2.50	2.14	1.12	0.00	0.00	0.00	0.00
50.	0.00	0.00	0.00	0.96	1.84	2.17	1.85	0.96	0.00	0.00	0.00	0.00
40.	0.00	0.00	0.00	0.78	1.49	1.76	1.50	0.79	0.00	0.00	0.00	0.00
30.	0.00	0.00	0.00	0.59	1.10	1.30	1.10	0.59	0.00	0.00	0.00	0.00
20.	0.00	0.00	0.00	0.39	0.71	0.83	0.71	0.40	0.00	0.00	0.00	0.00
10.	0.00	0.00	0.00	0.20	0.34	0.39	0.34	0.20	0.00	0.00	0.00	0.00
0.	0.00	0.00	0.00	0.00	0.00	0.00	0.00	0.00	0.00	0.00	0.00	0.00

Appendix F (cont'd.) Rate constant for $NO_2 + h\nu \rightarrow NO + O(^3P)$ as a function of month and latitude
Units: 10^{-1} min^{-1} Local time: 0600

MONTH	1	2	3	4	5	6	7	8	9	10	11	12
LATITUDE												
90.	0.00	0.00	0.00	0.78	1.48	1.73	1.49	0.79	0.00	0.00	0.00	0.00
80.	0.00	0.00	0.64	1.59	2.21	2.41	2.23	1.61	0.65	0.00	0.00	0.00
70.	0.00	0.52	1.45	2.30	2.77	2.92	2.79	2.32	1.47	0.52	0.00	0.00
60.	0.62	1.32	2.19	2.84	3.19	3.29	3.20	2.86	2.21	1.33	0.63	0.40
50.	1.44	2.08	2.77	3.24	3.48	3.56	3.49	3.26	2.79	2.10	1.44	1.18
40.	2.19	2.69	3.19	3.52	3.68	3.72	3.69	3.53	3.20	2.70	2.19	1.97
30.	2.77	3.14	3.49	3.71	3.79	3.81	3.80	3.72	3.50	3.15	2.78	2.61
20.	3.20	3.46	3.69	3.81	3.84	3.83	3.84	3.82	3.70	3.46	3.20	3.08
10.	3.50	3.67	3.81	3.84	3.80	3.78	3.81	3.84	3.81	3.67	3.50	3.42
0.	3.70	3.80	3.85	3.80	3.69	3.64	3.69	3.80	3.85	3.80	3.70	3.65

Appendix F. (cont'd.) Rate constant for $HNO_2 + h\nu \rightarrow NO + OH$ as a function of month and latitude
Units: 10^{-2} min^{-1} Local time: 1200

LATITUDE	MONTH 1	2	3	4	5	6	7	8	9	10	11	12
90	0.00	0.00	0.00	0.78	1.48	1.73	1.49	0.79	0.00	0.00	0.00	0.00
80	0.00	0.00	0.43	1.35	2.00	2.22	2.01	1.36	0.44	0.00	0.00	0.00
70	0.00	0.15	0.96	1.87	2.42	2.59	2.43	1.89	0.97	0.15	0.00	0.00
60	0.10	0.63	1.51	2.29	2.72	2.86	2.74	2.31	1.53	0.64	0.10	0.00
50	0.59	1.20	2.00	2.61	2.94	3.05	2.95	2.63	2.01	1.21	0.59	0.39
40	1.18	1.75	2.38	2.84	3.08	3.15	3.09	2.85	2.40	1.76	1.19	0.97
30	1.76	2.20	2.67	2.99	3.14	3.18	3.14	3.00	2.68	2.21	1.76	1.58
20	2.24	2.56	2.87	3.06	3.13	3.14	3.13	3.06	2.87	2.56	2.24	2.10
10	2.61	2.81	2.98	3.05	3.04	3.02	3.04	3.05	2.99	2.81	2.61	2.52
0	2.87	2.97	3.02	2.97	2.87	2.81	2.87	2.97	3.02	2.97	2.87	2.82

Appendix F. (cont'd.) Rate constant for $HNO_2 + h\nu \rightarrow NO + OH$ as a function of month and latitude
Units: 10^{-2} min^{-1} Local time: 0900

MONTH	1	2	3	4	5	6	7	8	9	10	11	12
LATITUDE												
90	0.00	0.00	0.00	0.78	1.48	1.73	1.49	0.79	0.00	0.00	0.00	0.00
80	0.00	0.00	0.00	0.76	1.46	1.71	1.47	0.77	0.00	0.00	0.00	0.00
70	0.00	0.00	0.00	0.72	1.38	1.62	1.39	0.73	0.00	0.00	0.00	0.00
60	0.00	0.00	0.00	0.66	1.26	1.48	1.26	0.66	0.00	0.00	0.00	0.00
50	0.00	0.00	0.00	0.57	1.09	1.28	1.09	0.58	0.00	0.00	0.00	0.00
40	0.00	0.00	0.00	0.47	0.88	1.04	0.88	0.47	0.00	0.00	0.00	0.00
30	0.00	0.00	0.00	0.36	0.65	0.77	0.66	0.36	0.00	0.00	0.00	0.00
20	0.00	0.00	0.00	0.24	0.43	0.50	0.43	0.24	0.00	0.00	0.00	0.00
10	0.00	0.00	0.00	0.12	0.21	0.24	0.21	0.12	0.00	0.00	0.00	0.00
0	0.00	0.00	0.00	0.00	0.00	0.00	0.00	0.00	0.00	0.00	0.00	0.00

Appendix F. (cont'd.) Rate constant for $HNO_2 + h\nu \rightarrow NO + OH$ as a function of month and latitude
Units: 10^{-2} min^{-1} Local time: 0600

MONTH	1	2	3	4	5	6	7	8	9	10	11	12
LATITUDE												
90.	0.00	0.00	0.00	0.25	0.52	0.63	0.54	0.27	0.00	0.00	0.00	0.00
80.	0.00	0.00	0.20	0.56	0.83	0.94	0.86	0.60	0.22	0.00	0.00	0.00
70.	0.00	0.16	0.51	0.87	1.11	1.21	1.15	0.92	0.54	0.17	0.00	0.00
60.	0.20	0.46	0.83	1.15	1.35	1.42	1.38	1.21	0.88	0.48	0.21	0.12
50.	0.52	0.80	1.13	1.38	1.53	1.59	1.57	1.44	1.18	0.83	0.53	0.42
40.	0.86	1.11	1.38	1.57	1.67	1.71	1.70	1.62	1.43	1.15	0.88	0.77
30.	1.18	1.38	1.58	1.71	1.77	1.79	1.80	1.75	1.63	1.41	1.20	1.10
20.	1.44	1.59	1.73	1.81	1.83	1.83	1.84	1.84	1.77	1.62	1.45	1.38
10.	1.64	1.75	1.83	1.85	1.83	1.81	1.83	1.86	1.85	1.76	1.65	1.59
0.	1.78	1.84	1.87	1.83	1.76	1.72	1.76	1.83	1.87	1.84	1.78	1.75

Appendix F. (cont'd.) Rate constant for $H_2O_2 + h\nu \rightarrow 2OH$ as a function of month and latitude
Units: 10^{-3} min^{-1} Local time: 1200

MONTH	1	2	3	4	5	6	7	8	9	10	11	12
LATITUDE												
90	0.00	0.00	0.00	0.25	0.52	0.63	0.54	0.27	0.00	0.00	0.00	0.00
80	0.00	0.00	0.13	0.46	0.74	0.85	0.77	0.49	0.14	0.00	0.00	0.00
70	0.00	0.04	0.32	0.68	0.93	1.03	0.96	0.72	0.34	0.04	0.00	0.00
60	0.02	0.20	0.53	0.88	1.10	1.18	1.13	0.92	0.57	0.21	0.03	0.00
50	0.19	0.42	0.75	1.04	1.22	1.29	1.25	1.09	0.79	0.44	0.20	0.12
40	0.42	0.65	0.94	1.18	1.31	1.36	1.34	1.22	0.98	0.68	0.43	0.34
30	0.67	0.88	1.11	1.28	1.37	1.40	1.39	1.31	1.14	0.90	0.69	0.60
20	0.91	1.07	1.23	1.34	1.38	1.39	1.39	1.36	1.26	1.09	0.92	0.85
10	1.11	1.22	1.32	1.35	1.34	1.34	1.35	1.36	1.33	1.23	1.12	1.07
0	1.27	1.32	1.35	1.31	1.25	1.22	1.25	1.31	1.35	1.32	1.27	1.24

Appendix F. (cont'd.) Rate constant for $H_2O_2 + h\nu \rightarrow 2OH$ as a function of month and latitude
Units: 10^{-3} min^{-1} Local time: 0900

MONTH	1	2	3	4	5	6	7	8	9	10	11	12
LATITUDE												
90.	0.00	0.00	0.00	0.25	0.52	0.63	0.54	0.27	0.00	0.00	0.00	0.00
80.	0.00	0.00	0.00	0.24	0.51	0.62	0.53	0.26	0.00	0.00	0.00	0.00
70.	0.00	0.00	0.00	0.23	0.48	0.58	0.49	0.25	0.00	0.00	0.00	0.00
60.	0.00	0.00	0.00	0.21	0.43	0.53	0.45	0.22	0.00	0.00	0.00	0.00
50.	0.00	0.00	0.00	0.18	0.37	0.45	0.38	0.19	0.00	0.00	0.00	0.00
40.	0.00	0.00	0.00	0.15	0.30	0.36	0.30	0.15	0.00	0.00	0.00	0.00
30.	0.00	0.00	0.00	0.11	0.22	0.26	0.22	0.11	0.00	0.00	0.00	0.00
20.	0.00	0.00	0.00	0.07	0.14	0.16	0.14	0.07	0.00	0.00	0.00	0.00
10.	0.00	0.00	0.00	0.03	0.06	0.07	0.06	0.03	0.00	0.00	0.00	0.00
0	0.00	0.00	0.00	0.00	0.00	0.00	0.00	0.00	0.00	0.00	0.00	0.00

Appendix F. (cont'd.) Rate constant for $H_2O_2 + h\nu \rightarrow 2OH$ as a function of month and latitude
Units: 10^{-3} min^{-1} Local time: 0600

MONTH	1	2	3	4	5	6	7	8	9	10	11	12
LATITUDE												
90.	0.00	0.00	0.00	0.24	0.54	0.68	0.58	0.27	0.00	0.00	0.00	0.00
80.	0.00	0.00	0.19	0.59	0.93	1.08	0.99	0.66	0.22	0.00	0.00	0.00
70.	0.00	0.15	0.53	0.98	1.31	1.45	1.38	1.09	0.60	0.17	0.00	0.00
60.	0.19	0.48	0.94	1.37	1.64	1.76	1.72	1.48	1.04	0.53	0.21	0.11
50.	0.56	0.90	1.34	1.71	1.93	2.03	2.01	1.83	1.46	0.98	0.59	0.45
40.	1.01	1.34	1.71	2.00	2.16	2.23	2.23	2.11	1.83	1.42	1.05	0.89
30.	1.46	1.74	2.04	2.24	2.33	2.37	2.38	2.33	2.14	1.81	1.50	1.35
20.	1.85	2.07	2.29	2.41	2.43	2.44	2.47	2.47	2.36	2.13	1.88	1.76
10.	2.17	2.33	2.47	2.49	2.45	2.42	2.46	2.52	2.50	2.36	2.18	2.10
0.	2.40	2.50	2.53	2.47	2.35	2.29	2.35	2.47	2.53	2.50	2.40	2.35

Appendix F. (cont'd.) Rate constant for $HCHO + h\nu \rightarrow H + HCO$ as a function of month and latitude
Units: 10^{-3} min^{-1} Local time: 1200

MONTH	1	2	3	4	5	6	7	8	9	10	11	12
LATITUDE												
90	0.00	0.00	0.00	0.24	0.54	0.68	0.58	0.27	0.00	0.00	0.00	0.00
80	0.00	0.00	0.11	0.47	0.81	0.96	0.87	0.53	0.13	0.00	0.00	0.00
70	0.00	0.03	0.31	0.74	1.07	1.21	1.13	0.81	0.36	0.03	0.00	0.00
60	0.02	0.19	0.57	0.99	1.29	1.42	1.35	1.08	0.63	0.21	0.02	0.00
50	0.18	0.44	0.84	1.23	1.48	1.58	1.54	1.32	0.92	0.47	0.20	0.11
40	0.45	0.73	1.11	1.43	1.62	1.70	1.67	1.51	1.19	0.78	0.47	0.36
30	0.77	1.03	1.34	1.59	1.72	1.77	1.76	1.65	1.41	1.08	0.79	0.68
20	1.10	1.31	1.54	1.69	1.75	1.77	1.78	1.74	1.59	1.35	1.11	1.01
10	1.38	1.54	1.67	1.73	1.71	1.70	1.72	1.74	1.69	1.55	1.39	1.32
0	1.61	1.69	1.73	1.67	1.58	1.53	1.58	1.67	1.73	1.69	1.61	1.57

Appendix F. (cont'd.) Rate constant for $HCHO + h\nu \rightarrow H + HCO$ as a function of month and latitude
Units: 10^{-3} min^{-1} Local time: 0900

MONTH	1	2	3	4	5	6	7	8	9	10	11	12
LATITUDE												
90	0.00	0.00	0.00	0.24	0.54	0.68	0.58	0.27	0.00	0.00	0.00	0.00
80	0.00	0.00	0.00	0.23	0.53	0.67	0.57	0.26	0.00	0.00	0.00	0.00
70	0.00	0.00	0.00	0.22	0.50	0.63	0.53	0.25	0.00	0.00	0.00	0.00
60	0.00	0.00	0.00	0.20	0.45	0.56	0.47	0.22	0.00	0.00	0.00	0.00
50	0.00	0.00	0.00	0.17	0.38	0.48	0.40	0.19	0.00	0.00	0.00	0.00
40	0.00	0.00	0.00	0.14	0.30	0.38	0.31	0.15	0.00	0.00	0.00	0.00
30	0.00	0.00	0.00	0.10	0.22	0.27	0.22	0.11	0.00	0.00	0.00	0.00
20	0.00	0.00	0.00	0.06	0.13	0.16	0.13	0.06	0.00	0.00	0.00	0.00
10	0.00	0.00	0.00	0.02	0.05	0.06	0.05	0.03	0.00	0.00	0.00	0.00
0	0.00	0.00	0.00	0.00	0.00	0.00	0.00	0.00	0.00	0.00	0.00	0.00

Appendix F. (cont'd.) Rate constant for $HCHO + h\nu \rightarrow H + HCO$ as a function of month and latitude
Units: 10^{-3} min^{-1} Local time: 0600

MONTH	1	2	3	4	5	6	7	8	9	10	11	12
LATITUDE												
90.	0.00	0.00	0.00	0.19	0.59	0.83	0.70	0.27	0.00	0.00	0.00	0.00
80.	0.00	0.00	0.14	0.66	1.25	1.55	1.43	0.87	0.21	0.00	0.00	0.00
70.	0.00	0.10	0.58	1.33	1.98	2.30	2.22	1.65	0.78	0.14	0.00	0.00
60.	0.16	0.53	1.27	2.10	2.72	3.02	2.98	2.50	1.59	0.66	0.18	0.08
50.	0.68	1.25	2.10	2.88	3.42	3.69	3.70	3.32	2.50	1.49	0.76	0.52
40.	1.52	2.16	2.97	3.63	4.04	4.25	4.29	4.05	3.39	2.45	1.64	1.32
30.	2.51	3.12	3.81	4.31	4.56	4.69	4.77	4.66	4.19	3.40	2.64	2.30
20.	3.48	4.01	4.55	4.84	4.92	4.96	5.06	5.09	4.83	4.24	3.60	3.30
10.	4.34	4.75	5.09	5.16	5.03	4.97	5.09	5.26	5.21	4.85	4.39	4.16
0.	4.97	5.23	5.32	5.11	4.77	4.61	4.77	5.11	5.32	5.23	4.97	4.84

Appendix F. (cont'd.) Rate constant for $CH_3CHO + h\nu \rightarrow CH_3 + HCO$ as a function of month and latitude
Units: 10^{-4} min^{-1} Local time: 1200

MONTH	1	2	3	4	5	6	7	8	9	10	11	12
LATITUDE												
90.	0.00	0.00	0.00	0.19	0.59	0.83	0.70	0.27	0.00	0.00	0.00	0.00
80	0.00	0.00	0.06	0.49	1.03	1.32	1.19	0.65	0.10	0.00	0.00	0.00
70.	0.00	0.01	0.28	0.90	1.50	1.80	1.69	1.13	0.39	0.01	0.00	0.00
60	0.00	0.15	0.65	1.37	1.96	2.25	2.17	1.65	0.83	0.20	0.01	0.00
50	0.15	0.47	1.12	1.85	2.40	2.66	2.61	2.16	1.37	0.58	0.17	0.08
40	0.52	0.97	1.66	2.32	2.76	2.97	2.95	2.61	1.93	1.12	0.57	0.40
30	1.09	1.58	2.21	2.73	3.04	3.18	3.19	2.97	2.45	1.74	1.16	0.94
20	1.77	2.20	2.70	3.04	3.19	3.25	3.29	3.21	2.88	2.34	1.83	1.61
10	2.42	2.76	3.07	3.18	3.14	3.12	3.18	3.25	3.14	2.82	2.45	2.29
0	2.97	3.15	3.22	3.07	2.84	2.73	2.84	3.07	3.22	3.15	2.97	2.88

Appendix F. (cont'd.) Rate constant for $CH_3CHO + h\nu \rightarrow CH_3 + HCO$ as a function of month and latitude
Units: 10^{-4} min^{-1} Local time: 0900

MONTH	1	2	3	4	5	6	7	8	9	10	11	12
LATITUDE												
90	0.00	0.00	0.00	0.19	0.59	0.83	0.70	0.27	0.00	0.00	0.00	0.00
80	0.00	0.00	0.00	0.18	0.58	0.81	0.68	0.25	0.00	0.00	0.00	0.00
70	0.00	0.00	0.00	0.17	0.54	0.75	0.62	0.23	0.00	0.00	0.00	0.00
60	0.00	0.00	0.00	0.15	0.47	0.66	0.54	0.20	0.00	0.00	0.00	0.00
50	0.00	0.00	0.00	0.13	0.39	0.54	0.44	0.16	0.00	0.00	0.00	0.00
40	0.00	0.00	0.00	0.10	0.29	0.40	0.32	0.12	0.00	0.00	0.00	0.00
30	0.00	0.00	0.00	0.06	0.19	0.26	0.21	0.07	0.00	0.00	0.00	0.00
20	0.00	0.00	0.00	0.03	0.10	0.13	0.10	0.04	0.00	0.00	0.00	0.00
10	0.00	0.00	0.00	0.01	0.03	0.04	0.03	0.01	0.00	0.00	0.00	0.00
0	0.00	0.00	0.00	0.00	0.00	0.00	0.00	0.00	0.00	0.00	0.00	0.00

Appendix F. (cont'd.) Rate constant for $CH_3CHO + h\nu \rightarrow CH_3 + HCO$ as a function of month and latitude
Units: 10^{-4} min^{-1} Local time: 0600